

# **Experimental Investigation & Optimization of Pulse Current TIG Welding Parameter For AA5052 & AA6063 Dissimilar Weld Joint**

SubmittedBy

**CHAVDA JAYDEEPKUMAR ARVINDBHAI**

**(210044002)**

SupervisedBy

**Mr. Sagarkumar I. Shah**

Assistant Professor

Mechanical Engineering Department

Atmiya University

A Thesis Submitted to

ATMIYA UNIVERSITY in Partial Fulfillment of the Requirements for

the Degree of Master of Technology in

Mechanical Engineering (Production)



**Faculty of Engineering & Technology,  
Mechanical Engineering Department,**

**ATMIYA UNIVERSITY**

**Yogidham Gurukul, Kalawad Road Rajkot, 360005**

**MAY – 2023**

## **Certificate**

It is certified that the work contained in the dissertation thesis entitled "**Experimental Investigation & Optimization of Pulse Current TIG Welding Parameter For AA5052 & AA6063 Dissimilar Weld Joint**" submitted by **CHAVDA JAYDEEPKUMAR A. (21044002)**, studying at Mechanical Engineering Department, Faculty of Engineering & Technology, for the award of M.Tech (Production Engineering) is absolutely based on his own work carried out under my supervision and this thesis has not been submitted elsewhere for any degree.

Date:

Place:

**Mr. Sgarkumar I. Shah**  
Assistant Professor,  
Mechanical Engineering Department

**Manojkumar Sheladiya**  
Head of Department  
Mechanical Engineering Department

**Signature and Name of external supervisor**

**Seal of University**

## **COMPLIANCE REPORT**

It is certified that the work contained in this dissertation thesis entitled “**Experimental Investigation & Optimization Of Pulse Current TIG Welding Parameter For AA5052 & AA6063 Dissimilar Weld Joint**” submitted by **Mr. CHAVDA JAYDEEPKUMAR A. (210044002)** studying at Mechanical Engineering Department, Faculty of Engineering & Technology for partial fulfilment of M.Tech degree to be awarded by Atmiya University. He has complied the comments of the Dissertation Progress Review-I, Mid Semester Dissertation as well as Dissertation Progress Review-II with my satisfaction.

**Date:**

**Place: Rajkot**

**Chavda Jaydeepkumar A.  
210044002**

**Mr. Sagarkumar I. Shah,  
Assistant professor,  
Mechanical Engg. Department,  
Atmiya University, Rajkot.**

**Signature and name of external supervisor**

## **PAPER PUBLICATION CERTIFICATE**

This is to certify that research work embodied in this dissertation titled **“Experimental Investigation & Optimization Of Pulse Current TIG Welding Parameter For AA5052 & AA6063 Dissimilar Weld Joint”** was carried out by **CHAVDA JAYDEEPKUMAR A. (En.No. 210044002)** at **Faculty of Engineering & Technology, Rajkot** for partial fulfillment of Master of Technology degree to be awarded by Atmiya University has published review article **“Weldability of Aluminium Alloy Using Tungsten Inert Gas Welding Process for Mechanical Properties: A Review”** for publication in the **“Trends in Materials & Metallurgical Engineering, Volume 13 Issue 1, 2023.”**

**Date:**

**Place: Rajkot**

**Jaydeepkumar Chavda  
210044002**

**Mr. Sagarkumar I. Shah,  
Assistant professor,  
Mechanical Engg. Department,  
Atmiya University, Rajkot.**

**Signature and name of external supervisor**

**Seal of University**

## **THESIS APPROVAL CERTIFICATE**

It is certified that the work contained in this dissertation thesis is entitled "**Experimental Investigation & Optimization Of Pulse Current TIG Welding Parameter For AA5052 & AA6063 Dissimilar Weld Joint**" submitted by **Mr. Jaydeepkumar Chavda (210044002)** studying at Mechanical Engineering Department, Faculty of Engineering & Technology for partial fulfilment of M.Tech degree to be awarded by Atmiya University.

**Date:**

**Place: Rajkot**

External Examiners Sign and Name:

1) \_\_\_\_\_

## **DECLARATION OF ORIGINALITY**

We hereby certify that we are the sole authors of this thesis and that neither any part of this thesis nor the whole of the thesis has been submitted for a degree to any other University.

We certify that, to the best of our knowledge, the current thesis does not infringe upon anyone's copyright nor violate any proprietary rights and that any ideas, techniques, quotations or any other material from the work of other people included in our thesis, published or otherwise, are fully acknowledged in accordance with the standard referencing practices. Furthermore, to the extent that we have included copyrighted material that surpasses the boundary of fair dealing within the meaning of the Indian Copyright (Amendment) Act 2012, we certify that we have obtained a written permission from the copyright owner(s) to include such material(s) in the current thesis and have included copies of such copyright clearances to our appendix.

We declare that this is a true copy of thesis, including any final revisions, as approved by thesis review committee.

We have checked write up of the present thesis using anti-plagiarism database and it is in allowable limit. Even though later on in case of any complaint pertaining of plagiarism, we are solely responsible for the same and we understand that as per UGC norms, University can even revoke Master of Technology degree conferred to the student submitting this thesis.

**Date:**

**Place: Rajkot**

**Student Signature: \_\_\_\_\_ Signature of Guide: \_\_\_\_\_**

**Name of Student: Jaydeepkumar Chavda Name of Guide: Mr. Sagar I. Shah**

**Enrollment No: 210044002**

## **ACKNOWLEDGEMENT**

I wish to express my sincere gratitude and regards to my project guide, **Mr. Sagarkumar I. Shah (Asst. Prof. Mechanical Engineering Department Atmiya University, Rajkot)** his guidance and support throughout the program has been a major factor in the successful completion of the present work. This work would not have culminated into the present form without his valuable suggestions and generous help. I am thankful to **Dr. G. D. Acharya (Professor Emeritus, Atmiya University, Rajkot), Mr. Manojkumar Sheladiya(Head of Mechanical Engineering Department, Atmiya University, Rajkot)** and also **Dr. Pratik T. Kikani (Asst. Prof. Mechanical Engineering Department)** for continuous guidance & inspiration throughout by PG program.

I am also thankful to workshop staff **Mr. Marubhai** of Atmiya University for continuous helping for completion of dissertation work.

I am thankful to all faculty members and friends at **ATMIYA UNIVERSITY, RAJKOT** who not only provided valuable suggestions and constant help during my work.

Above all, I am forever thankful to my mother for her valuable time and encouragement.

## TABLE OF CONTENT

SR.NO.	CONTENT	PAGE NO
	Title page	
	Certificate	
	Compliance report	
	Paper Publication certificate	
	Thesis approval Certificate	
	Declaration of originality	
	Acknowledgement	
	Table of content	
	List of Figures	
	List of Table	
	Nomenclature	
	Abstract	
<b>CHAPTER-1</b>	<b>Introduction to material</b>	
1.1	Aluminum	
1.2	Aluminum alloy grades	
1.2.1	1000 series alloy	
1.2.2	2000 series alloy	
1.2.3	3000 series alloy	
1.2.4	4000 series alloy	
1.2.5	5000 series alloy	
1.2.6	6000 series alloy	
1.2.7	7000 series alloy	
1.3	AA5052 & AA6063 dissimilar weld joint application	
1.3.1	Marine application	
1.3.1.1	Deck	



1.3.1.2	Hull	
1.3.1.3	Keel	
1.3.1.4	Bulkhead	
<b>CHAPTER-2</b>	<b>Introduction to welding process</b>	
2.1	Background	
2.1.1	Welding	
2.1.2	Definition	
2.2	Classification of welding process	
2.3	Weldability	
2.3.1	Factor affecting weldability	
2.4	Tungsten inert gas welding process	
2.4.1	Welding current	
2.4.2	Welding speed	
2.4.3	Gas flow rate	
2.4.4	Welding voltage	
2.5	Constant process parameters	
2.6	Operating input parameters	
2.7	Operating output parameters	
<b>CHAPTER-3</b>	<b>Literature review</b>	
3.1	Literature review	
3.2	Literature summary	
3.3	Problem identification	
3.4	Research objective	
<b>CHAPTER-4</b>	<b>Methodology</b>	
4.1	Flow of entire work	
4.2	Parameters selection for work	
4.3	Range of parameters	
<b>CHAPTER-5</b>	<b>Design of experiments</b>	

5.1	Experimental design	
5.2	Central composite design	
5.3	Design of experiments (D.O.E.)	
<b>CHAPTER-6</b>	<b>Experimental work</b>	
6.1	Appratus	
6.1.1	Base material	
6.2	Consumable and electrode	
6.3	Joint design of weld	
6.4	Weld preparation	
6.5	Performing experiment	
6.6	Welded specimens	
6.7	Liquid penetrant test	
6.7.1	Inspection steps for liquid penetrant test	
6.7.1.1	Pre – cleaning	
6.7.1.2	Penetrant application	
6.7.1.3	Excess penetrant removal	
6.7.1.4	Developer application	
6.7.1.5	Inspection	
6.7.1.6	Post – cleaning	
6.7.2	Advantages	
6.7.3	Disadvantages	
6.8	Observation after liquid penetrant test	
6.9	Hardness testing	
6.10	Tensile testing	
<b>CHAPTER-7</b>	<b>Result and discussion</b>	
7.1	Actual experiment results	
7.1.1	Liquid penetrant test result	
7.1.2	Hardness test result	

7.1.2.1	3D surface plot for hardness	
7.1.3	Tensile test result	
7.1.3.1	3D surface plot of peak current and base current for tensile	
7.1.3.2	3D surface plot of peak current and pulse per second for tensile	
7.1.3.3	3D surface plot of base current and pulse per second for tensile	
<b>CHAPTER-8</b>	<b>Optimization and validation</b>	
8.1	Optimization using response surface method	
8.2	Experimental design and data collection	
8.3	Model fitting	
8.3.1	Regression analysis	
8.3.2	Regression equation of hardness	
8.3.3	Regression equation of tensile	
8.4	Model analysis	
8.4.1	ANOVA for hardness (WZ)	
8.4.2	ANOVA for tensile strength	
8.5	Model optimization	
8.6	Validation of results	
<b>CHAPTER-9</b>	<b>Conclusions and future scope</b>	
9.1	Conclusions	
9.2	Future scope	
	<b>References</b>	
	<b>APPENDIX A:Review card</b>	
	<b>APPENDIX B:Compliance Report</b>	
	<b>APPENDIX C:Paper Publication certificate</b>	
	<b>APPENDIX D: Material test report</b>	
	<b>APPENDIX E: ASME codes and standards</b>	
	<b>APPENDIX F: Welding procedure specification</b>	
	<b>APPENDIX E: plagiarism</b>	

## List of Figures

<b>SR.NO.</b>	<b>FIGURE</b>	<b>PAGE NO</b>
FIG 1.1	ER 4043 filler wire	
FIG 1.2	Main structural parts of ships	
FIG 2.1	Classification of welding	
FIG 2.2	Tungsten inert gas welding process	
FIG 6.1	Base metal AA6063 aluminum alloy	
FIG 6.2	Base metal AA5052 aluminum alloy	
FIG 6.3	ER 4043 filler wire	
FIG 6.4	Joint design	
FIG 6.6	Included angle 60	
FIG 6.7	TIG welding machine setup	
FIG 6.8	Performing welding experiment	
FIG 6.9	Welded specimens	
FIG 6.10	Application of penetrant on specimen	
FIG 6.11	Application of developer on specimen	
FIG 6.12	Hardness testing machine	
FIG 6.13	Performing hardness test	
FIG 6.14	Tensile test specimen ASTM 370 standard	
FIG 6.15	Preparing tensile test specimen using Hacksaw cutting machine	
FIG 6.16	Tensile test specimens	
FIG 6.17	Tensile test on UTM	
FIG 6.18	Performing tensile testing	
FIG 7.1	3D surface plot for hardness	
FIG 7.2	3D surface plot of peak current and base current for tensile	
FIG 7.3	3D surface plot of peak current and pulse per second for tensile	
FIG 7.4	3D surface plot of base current and pulse per second for tensile	

## List of Tables

<b>SR.NO.</b>	<b>TABLE</b>	<b>PAGE NO</b>
	<b>Table of content</b>	
	<b>List of figures</b>	
	<b>List of tables</b>	
TABLE 1.1	AA5052 chemical composition	
TABLE 1.2	AA5052 mechanical properties	
TABLE 1.3	AA5052 physical properties	
TABLE 1.4	AA6063 chemical composition	
TABLE 1.5	AA6063 mechanical properties	
TABLE 1.6	AA6063 physical properties	
TABLE 1.7	Chemical composition of ER4043	
TABLE 2.1	Constant process parameters	
TABLE 4.1	Range of parameters	
TABLE 5.1	Experimental combination from design expert software	
TABLE 6.1	Observation after liquid penetrant test	
TABLE 7.1	Result of liquid penetrant test	
TABLE 7.2	Hardness test result	
TABLE 7.3	Tensile test result	
TABLE 8.1	Experimental design and data collection	
TABLE 8.2	ANOVA for hardness (WZ)	
TABLE 8.3	ANOVA for tensile strength	
TABLE 8.4	Constraints in optimization	
TABLE 8.5	Suggested optimized solution	
TABLE 8.6	Confirmation test result	
TABLE 8.7	Comparison of predicted result with experimental results	
APPENDIX: A	Comments for DP - 1 & MSD	

## **NOMENCLATURE**

GTAW	Gastungstenarcwelding
ASME	Americansocietyofmechanicalengineers
AWS	Americanweldingsociety
TIG	Tungsteninert gas
AC	Alternativecurrent
DC	Directcurrent
LPT	Liquidpenetrant testing
LPI	Liquidpenetrantinspection
WPS	Weldingprocedurespecification
WZ	WeldZone

## **ABSTRACT**

The most essential kind of welding, particularly for the most challenging metals to weld, such as aluminum, is tungsten inert gas (TIG) welding. Aluminum alloys are now welded using the pulsed current TIG technique. The pulsed current TIG welding process is a modified version of TIG welding. Nowadays AA5052 and AA6063 dissimilar weld joints are used in different areas such as automobile and marine applications. This is why it needs to have significant mechanical properties and corrosion resistance. The most effective selection of the process parameters is essential for producing the desired mechanical and physical properties of the weldment. The ASME Section IX is used to choose the TIG welding's most important input parameters. In this research, the impact of various welding parameters such as Peak current, Base current, and Pulse per second is chosen. For dissimilar welding of AA5052 and AA6063, 8mm thick plate joints, ER4043 filler wire is utilized in this project work. To examine the mechanical properties and weld strength of the weld joints, respectively, a tensile test is performed. Regression analysis and central composite design (CCD) are used to determine the input parameter that has the greatest impact on the final result. The response surface optimizer optimizes the selected parameters. Once the optimization is complete, evaluate the final result. Utilizing DESIGN EXPERT software for experiment design, the response surface method is applied for optimization.

**Keywords:** Aluminum, AA5052, AA6063, Pulsed Current TIG Welding, Welding Procedure Specification, Tensile Strength, Hardness, Response Surface Method.

# CHAPTER - 1

## INTRODUCTION TO MATERIAL

---

### 1.1 Aluminum

Sir Humphrey Davy predicted the presence of aluminium (Al) in the first decade of the nineteenth century, and Hans Christian Oersted isolated the metal in 1825. When some limited commercial production started, it continued to be somewhat of a laboratory curiosity for the following 30 years, but it wasn't until 1886 that the extraction of aluminium from its mineral, bauxite, became a fully practical industrial process. Paul Heroult in France and Charles M. Hall in the United States concurrently developed the extraction technique, and this fundamental technology is still in use today.<sup>[1],[2]</sup>

Aluminium is reactive, therefore it does not naturally exist in its metallic state. Instead, it is found in the earth's crust in a variety of compounds, of which there are hundreds. The most significant and common is bauxite. The two steps of the extraction process are the separation of the aluminium oxide, Al<sub>2</sub>O<sub>3</sub> (alumina), from the ore and the electrolytic reduction of the alumina at temperatures between 950 and 1000 degrees Celsius in cryolite (Na<sub>3</sub>AlF<sub>6</sub>). This produces aluminium that contains 5–10% impurities like silicon (Si) and iron (Fe), which is subsequently purified either by an additional electrolytic process or using a zone-melting technique to produce a metal with a purity close to 99.9%.<sup>[1],[2]</sup>

At the end of the 20th century, a significant amount of aluminium was produced from recovered and remelted waste and scrap; in Europe (including the UK), this source alone produced about 2 million tonnes of aluminium alloys annually. Due to its relative weakness, the resultant pure metal is rarely employed, especially in construction-related applications. The pure aluminium is often alloyed with metals like copper (Cu), manganese (Mn), magnesium (Mg), silicon (Si), and zinc (Zn) to boost mechanical strength.<sup>[1],[2]</sup>



## 1.2 Aluminum Alloy Grades

There are various kinds of aluminium alloy grades that are utilized in various applications. The below lists various classes of aluminium along with their characteristics, uses, and primary alloying components or elements. It also specifies whether or not they can be heat treated.

### 1.2.1 1xxx series

The 1-series alloys are frequently employed in electrical and chemical applications and are typically thought of as soft alloys. It is offered in the form of tubes, pipes, rods, and wire. 99% of this alloy is aluminium, with the remaining 1% being another metal. The maximum amount of copper that can be added to this kind of metal is 0.12%. This alloy has good workability, excellent corrosion resistance, low mechanical properties, and strong electrical conductivity.<sup>[2]</sup>

### 1.2.2 2xxx series

This alloy, which has undergone heat treatment and is utilized for particular purposes, mostly contains copper as an alloying element. Because they are highly vulnerable to hot cracking, these alloys are very challenging to weld using an arc welding process. Therefore, by choosing the proper filler material and weld process parameters, these alloys can be joined using the arc welding process. High electrical conductivity and resistance to corrosion.<sup>[2]</sup>

### 1.2.3 3xxx series

The alloys from the 3 series fall within the category of soft alloys. It might be offered in the forms of sheets, plates, pipes, and tubes. The main alloying element in this alloy is manganese, though copper or magnesium are frequently added as well. This alloy is stronger, works well, and is largely corrosion resistant.<sup>[2]</sup>

### 1.2.4 4xxx series

This alloy, which has silicon as its primary alloying component and is available in both heat-treatable and non-heat-treatable forms, is frequently employed as filler

material. These alloys are frequently used as filler materials to unite different series of aluminium alloys, however caution must be exercised while welding them to other series alloys due of their high crack sensitivity.[2]

### **1.2.5 5xxx series**

When compared to other non-heat treatable aluminium alloys, this alloy has higher mechanical properties because magnesium is the main alloying element. As a result, these alloys are frequently utilised for structural purposes. Additionally, welding these alloys causes them to crack easily. As a result, while welding these metals, correct filler material and welding settings should be chosen.[2]

### **1.2.6 6xxx series**

This alloy, which is heat treatable, mostly consists of silicon and magnesium as alloying components. Without the filler, these alloys cannot be properly arc welded. Because of this, care should be taken when welding these alloys with 4xxx series and 5xxx series alloys to choose a filler material that will minimize the sensitivity of the weld metal fracture by reducing the amount of  $Mg_2Si$  in the base material.[2]

### **1.2.7 7xxx series**

The main alloying elements in this alloy are zinc, magnesium, and copper. Due to the possibility of hot fracture formation, these alloys are inappropriate for arc welding. Due to thermal pressures present during welding and varying degrees of solidification, the 7-series aluminum alloys develop hot cracking.[2]

**Table 1.1 AA5052ChemicalCompositions<sup>[3]</sup>**

<b>Elements</b>	<b>Al</b>	<b>Mg</b>	<b>Fe</b>	<b>Mn</b>	<b>Si</b>	<b>Cr</b>	<b>Cu</b>	<b>Zn</b>
<b>% Weight</b>	96.78	2.5	0.3	0.05	0.13	0.2	0.01	0.03

The chemical properties of the metal 5052 aluminum alloy, which is based on with ASME SECTION II PART A, are shown in Table 1.1 above. The mechanical properties of the metal 5052 aluminum alloy are listed in Table 1.2 below.

**Table 1.2 AA5052MechanicalProperties<sup>[4]</sup>**

MechanicalProperty	Value
Tensilestrength	195-290 Mpa
ProofStress	130Min Mpa
HardnessBrinell	61HB

The physical properties of the metal 5052 aluminium alloy are shown in Table 1.3 below.

**Table 1.3 AA5052PhysicalProperties<sup>[4]</sup>**

PhysicalProperty	Value
Density	2.68g/cm <sup>3</sup>
MeltingPoint	605 °C
ThermalExpansion	23.7*10 <sup>-6</sup> /K
ModulusOfElasticity	70Gpa
ThermalConductivity	138 W/m.K
ElectricalResistivity	0.0495*10 <sup>-6</sup> Ω.m

**Table 1.4 AA6063ChemicalCompositions<sup>[3]</sup>**

Elements	Al	Mg	Fe	Mn	Si	Cr	Cu	Zn
% Weight	96.78	0.45- 0.90	0.35	0.10	0.20- 0.60	0.2	0.10	0.10

The chemical properties of the metal 5052 aluminum alloy, which is based on ASME SECTION II PART A, are shown in Table 1.4 above. The mechanical properties of the metal 6063aluminum alloy are listed in Table 1.5 below.

**Table 1.5 AA6063MechanicalProperties<sup>[4]</sup>**

MechanicalProperty	Value
Tensilestrength	145-186Mpa
Yield strength	145 Mpa
HardnessBrinell	75HB

The physical properties of the metal 5052 aluminium alloy are shown in Table 1.6 below.

**Table 1.6 AA6063PhysicalProperties<sup>[4]</sup>**

PhysicalProperty	Value
Density	2.70g/cm <sup>3</sup>
MeltingPoint	582 °C
ThermalExpansion	23.5*10 <sup>-6</sup> /K
ModulusOfElasticity	70Gpa
ThermalConductivity	166 W/m.K
ElectricalResistivity	0.0495*10 <sup>-6</sup> Ω.m

2mm-diameter ER 4043 filler wire utilized in the current project is shown in Figure 1.2 below.



**Fig. 1.1 ER 4043 Filler wire<sup>[6]</sup>**

The chemical properties of the filler wire metal, ER4043 aluminium alloy, are listed in Table 1.7 below according to ASME SECTION II PART C. When welding aluminium parts, the 4043 aluminium alloy, a wrought alloy with good corrosion resistance, is frequently used as a filler material. Between 4.5 and 6.0% of it is silicon, and there are traces of other materials as well. Typically, 4043 will have a higher weldability rating and a marginally lower crack sensitivity rating.

**Table 1.7. Chemical composition of ER 4043<sup>[6]</sup>**

Content	Al	Si	Fe	Cu	Mg	Cr	Zn	Ti
% elements	93.84	5.82	0.09	0.02	<0.001	<0.001	<0.001	0.04

### 1.3 AA 5XXX & AA 6XXX dissimilar weld joint Application

#### 1.3.1 Marine Application<sup>[7]</sup>

There are some parts of a ship which is made from aluminum such as deck, hull, bulkhead, stiffeners, and keel. These parts are mostly made from aluminum 5XXX and 6XXX series respectively.

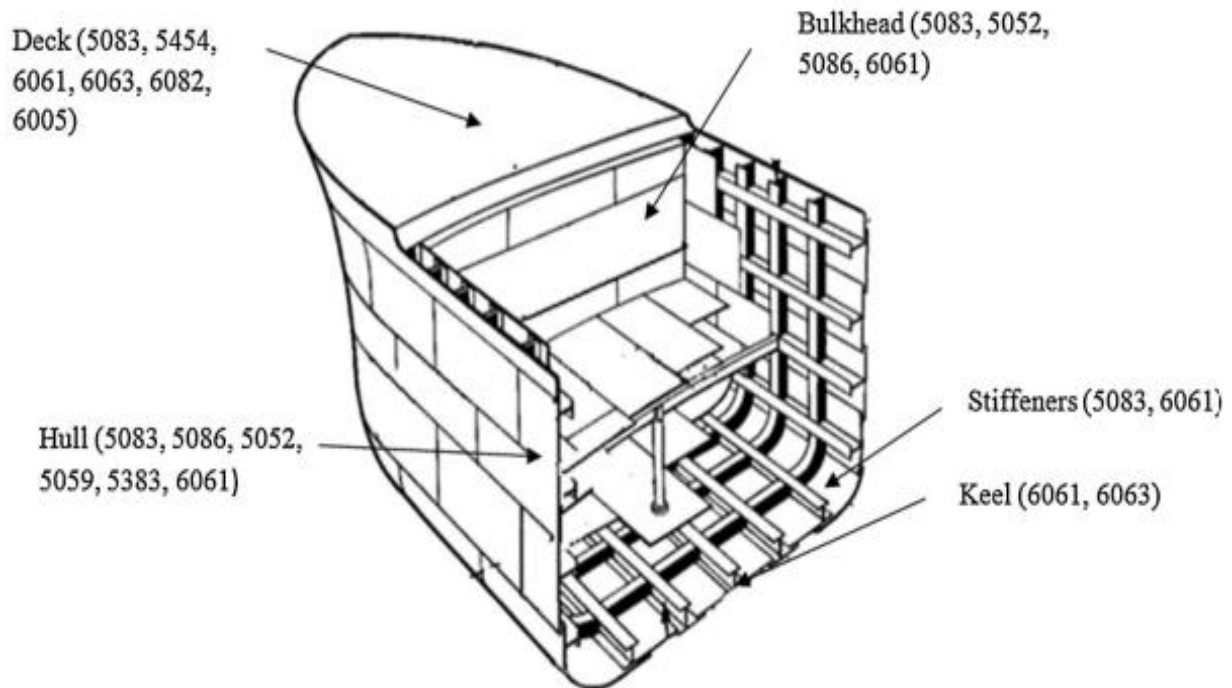


Fig. 1.2 Main structural parts of ships<sup>[7]</sup>

##### 1.3.1.1 Deck

Aluminum decks are becoming more and more common in modern shipbuilding because of their excellent strength-to-weight ratio, resistance to corrosion, and durability. Typically, an aluminum ship deck is made of an aluminum plate that is connected to a supporting framework through welding or other methods. To keep the plating from slipping in slick circumstances, it may be coated with anti-skid compounds. To direct water away from the working areas, the deck may also feature integrated drainage systems. The ability of an aluminum ship deck to reduce weight is one of its key benefits. Since aluminum is lighter than steel, less material is required to achieve an equivalent level of strength and performance. This makes the ship lighter, allowing it to move more quickly and efficiently. Excellent corrosion resistance is another benefit of aluminium decks, which is crucial in the marine

environment where elements like humidity, salinity, and other corrosives can cause damage over time. Additionally resistant to UV rays, which can fade and degrade other materials, is aluminium.

### **1.3.1.2 Hull**

As a result of its high strength-to-weight ratio, resistance to corrosion, and longevity, aluminum is a material that is being used for the building of ship hulls more and more frequently. Typically, the hull construction of an aluminum ship is created by welding together aluminum plates. Due to aluminum's lower yield strength, the plating is frequently thicker than that utilized in steel construction. Anti-corrosion coatings and anodes may be applied to the hull to lessen galvanic corrosion. The ability of an aluminum ship hull to reduce weight is one of its key benefits. Since aluminum is lighter than steel, less material is required to achieve an equivalent level of strength and performance. This makes the ship lighter, allowing it to move more quickly and efficiently.

### **1.3.1.3 Keel**

Aluminum keels are becoming more and more common in contemporary shipbuilding due to their excellent strength-to-weight ratio, resistance to corrosion, and durability. A conventional method of building an aluminum keel is to fuse aluminum plates or extrusions together to create the keel structure. The ability of an aluminum keel to reduce weight is one of its key benefits. Since aluminum is lighter than steel, less material is required to achieve an equivalent level of strength and performance. This makes the ship lighter, allowing it to move more quickly and efficiently. Excellent corrosion resistance is another benefit of aluminum keels, which is crucial in the marine environment where salt water, humidity, and other corrosive elements can gradually cause damage. Additionally resistant to UV rays, which can fade and degrade other materials, is aluminum.

### **1.3.1.4 Bulkhead**

Usually, the bulkhead structure of an aluminium bulkhead is created by welding aluminum plates or extrusions together. Due to aluminum's lower yield strength than steel, the thickness of the plates required for an aluminium bulkhead can be larger than that used for a steel bulkhead. The ability of an aluminium bulkhead to save

weight is one of its key benefits. Since aluminium is lighter than steel, less material is required to achieve an equivalent level of strength and performance. This makes the ship lighter, allowing it to move more quickly and efficiently. For vessels that experience frequent and severe stresses during their lifetime, aluminium bulkheads provide good fatigue resistance. They can also be repaired more quickly and inexpensively than steel bulkheads since aluminium is easily welded or replaced.

## CHAPTER - 2

### INTRODUCTION TO WELDING PROCESS

---

#### 2.1 Background:

In the modern world, manufacturing industries are essential to the growth of any nation. The prosperity of manufacturing firms determines the economic power of any developing nation. Additionally, the growth of the industrial sector can create additional job possibilities, which will help any nation prosper.

One of the most significant occurrences in the manufacturing area is joining. According to another definition, joining is "the joining of metals, either metal or non-metal, to serve some desired purpose," depending on the application. Depending on the application, joining techniques including welding, soldering, and brazing may be used.

The G.T.A.W welding process is the most used welding method for the production of household appliance goods. This technique is often used in industries since it is affordable, easy to use, and easily automatable.

#### 2.1.1 Welding

When bigger lengths of standard sections are needed or many pieces need to be linked together to build a desired structure, welding is one of the industrial methods that is typically used to combine metal parts. The process of combining metals and plastics without the use of adhesives or fasteners is known as welding.<sup>[1]</sup>

#### 2.1.2 Definition

Metal components are joined through the process of welding, which can be done with or without filler metal, pressure, or heat. Heat, pressure, and filler have all been used separately or in combination to create a variety of welding methods.<sup>[2]</sup>



## 2.2 Classification of Welding Processes

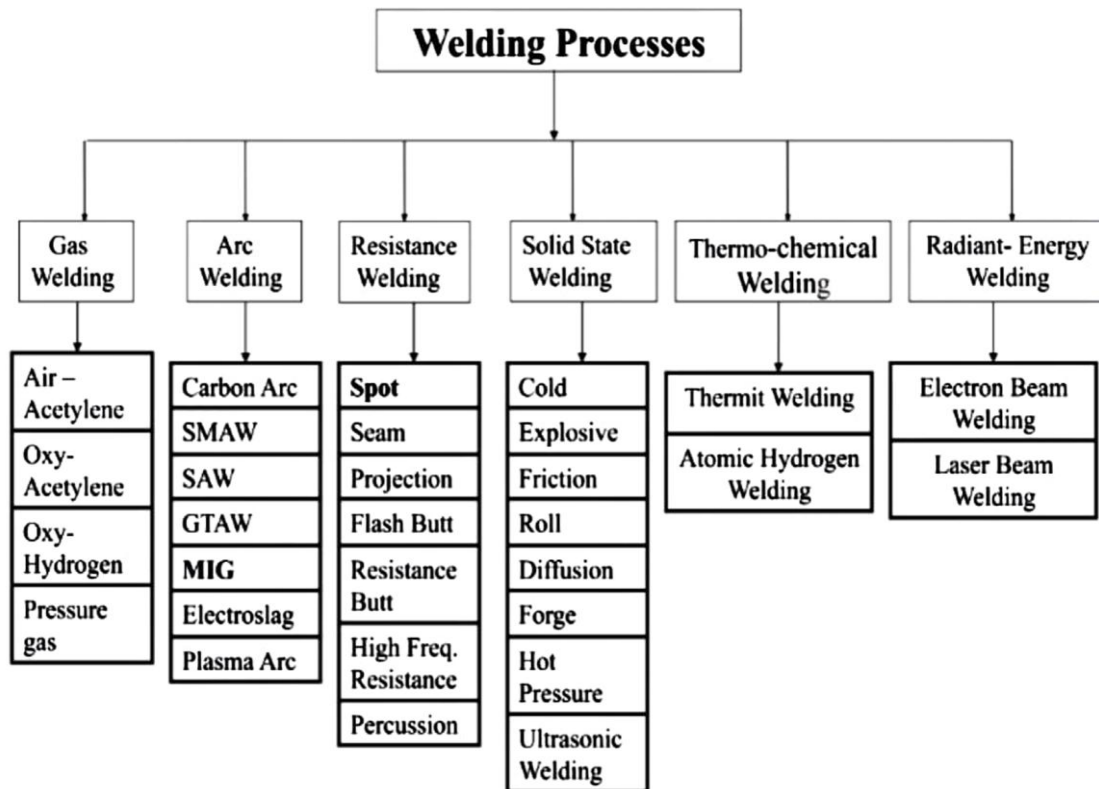


Fig 2.1- Classification of welding processes<sup>[8]</sup>

## 2.3 Weldability

Weldability has been defined as the capacity to be joined together by welding into inseparable joints with predetermined features, such as determined weld strength and an appropriate structure.<sup>[8]</sup>

There are five main aspects that affect the ability of a material to be welded:-

- Meltingpoint
- Thermalconductivity
- Thermalexpansion
- Surfacecondition
- Changeinthe microstructure.

The American Welding Society defines weldability as

**“weldability refers to how easily and reliably a material can be welded using a particular welding process to create a structure that performs well in its intended application. Weldability depends on various factors such as the chemical composition of the material, its physical properties, and the type of welding process being used.”<sup>[4]</sup>**

### 2.3.1 Factors Affecting Weldability

The weldability of metals is influenced by a number of factors. Some of the most significant ones are listed below.

- Metallurgy
- Welding Process
- Joint Design
- Weld Preparation
- Melting Point
- Electrical Resistance

## 2.4 Tungsten inert gas welding process

Since manual GTAW welding is totally dependent on the expertise of the craftsman, it is the most challenging of all the welding techniques generally used in industrial applications. When welding pressure vessels, welders must maintain a brief arc length to prevent electrode corrosion. For this reason, WPQ is necessary. The welder operates the welding torch as a weave bead while manually feeding filler metal into the weld zone with just one hand.

According to fig. 2.2, the GTAW welding technique is categorised as a fusion welding process. In this type of welding process, two metals, whether similar or dissimilar, join together using the parent metal.

In the fabrication industry, the technique of gas tungsten arc welding (GTAW) is the most well-liked and frequently used to create a variety of products. A non-consumable tungsten electrode is utilised to weld the components in the GTAW welding process.

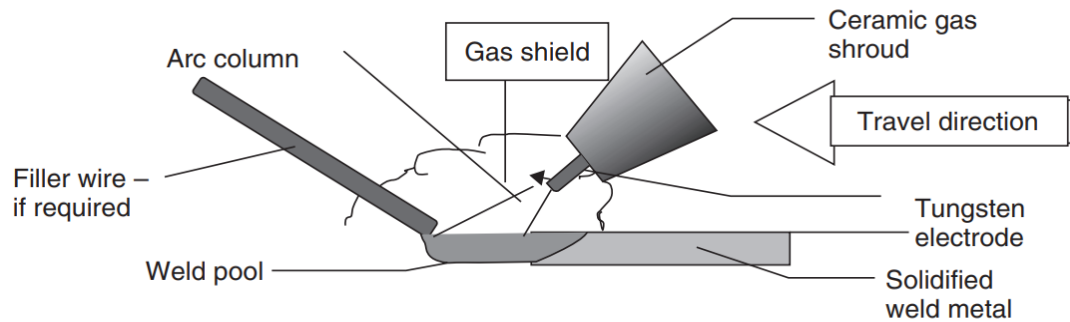


**Fig. 2.2- Tungsten inert gas welding process** <sup>[1]</sup>

It uses a variety of shielding gases, including argon, helium, or a combination of the two. Along with protecting against oxidation, the shielding gas also offers protection against other forms of pollution. Since argon is less expensive than helium, it is frequently used in the fabrication industry as a shielding gas. Helium is employed in contrast, but only when a deeper penetration is necessary. Depending on the application, filler wire may or may not be used during GTAW welding.

In order to join ferrous and non-ferrous components that are similar or different, this welding process is frequently used in the fabrication, chemical, and food processing industries as well as in the production of vessels, storage tanks, nuclear power plants, and pharmacy company plants.

#### **2.4.1 Welding Current:**

Higher current during the GTAW welding process can result in a defective work piece as well as undercut and spatter flaws on the joint side. Additionally, in the GTAW welding process, lower current settings make the torch stick to the base metal, preventing the base metal and filler wire from melting properly and producing an unattractive appearance. Typically, the fixed current mode will change the voltage while welding ferrous or nonferrous materials in order to maintain a consistent arc current. <sup>[1]</sup>

#### **2.4.2 Welding Speed:**

The welding speed is one of the most significant factors affecting a weld joint's

mechanical properties. As the speed increases, the heat input per unit length decreases, resulting in less penetration and reinforcement during welding. On the opposing side, fast welding creates undercut, weldment porosity, and irregular bead shapes. Slower welding speeds eliminate weld joint porosity defects and lack of fusion. <sup>[1]</sup>

### 2.4.3 Gas Flow Rate:

Whatever its purpose, inert gas flow rate is the most significant influencing parameter in the TIG welding process because it covers the weld bead from air contamination and prevents oxidation. The welding bead should weave while welding if the gas flow rate is high, while pinholes and porosity defects will develop if the gas flow rate is low. The fabrication sector frequently makes use of pure argon gas. There is a minor amount of use for other gases such as helium, carbon dioxide, and hydrogen. <sup>[1]</sup>

### 2.4.4 Welding Voltage:

The welding voltage might be fixed or adjustable depending on the GTAW welding machine and the thickness of the plate to be connected. Arc initiation is aided by a high initial voltage, and the rod does not adhere to the base metal or harm the plate. When compared to other procedures, excessive voltage can lead to a number of welding quality issues, including poor visual appeal and poor mechanical properties. <sup>[1]</sup>

## 2.5 Constant Process Parameters

**Table 2.1 Constant process parameters**

<b>Welding Machine</b>	Miller Dynasty 350
<b>Electrode material</b>	98% w + 2 % Zr
<b>Electrode diameter</b>	3.0 mm
<b>Filler wire material</b>	ER 4043
<b>Filler wire diameter</b>	2.0 mm
<b>Shielding gas</b>	Argon
<b>Gas flow rate</b>	10 lit/min
<b>Arc voltage</b>	12.5 – 20 volts

## **2.6 Operating Input Parameters**

- Peak Current
- Base Current
- Pulse Per Second

## **2.7 Operating output parameters**

- Tensile Strength
- Hardness

## CHAPTER – 3

### LITERATURE REVIEW

#### 3.1 Literature Review

**MOHD ATIF WAHID, ARSHAD NOOR SIDDIQUEE, ZAHID A. KHAN ET AL.[7]** The features and applications of various AAs now used in marine and shipbuilding constructions have been discussed in this research. Additionally, difficulties with AAs' weldability and corrosion in marine environments have been addressed. As aluminum is nearly three times lighter than steel, it allows transportation systems to operate at higher speeds and with greater loads while using less fuel and emitting fewer emissions. Due to their high strength-to-weight ratio and high corrosion resistance, AAs 5xxx and 6xxx are frequently used in the production of many different parts, including hulls, superstructures, deck panels, bulkheads, stack enclosures, keels, and gunwales for monohull vessels and superstructures used in marine environments. Corrosion is a serious issue with hull design and maintenance, which results in a loss of strength. Among the techniques for preventing corrosion brought on by the precipitation of  $\beta$ -phase particles are anodizing and cladding. To prevent corrosion, proper maintenance and inspection are necessary. It is challenging to combine heat-treatable and non-heat-treatable AAs using fusion welding techniques like GMAW and GTAW. This makes it possible to weld these metals using high-energy beam processes like laser welding.

**K.EAZHIL,S.MAHENDRAN,S.GANESHKUMARETAL.[11]** The Taguchi approach is applied in this paper to optimize tungsten inert gas welding on 6063 aluminium alloy. To maximize the mechanical qualities of weldments made from 6063 aluminium alloy, the Taguchi method L27 is employed to optimize the pulsed TIG welding process parameters. Finding the effects of certain components requires the use of an analysis of variance. The best settings for the TIG welding process are then identified, and the experimental findings support the suggested strategy.

**SANDEEPVERMA,H.K.ARYA,PANKAJKUMARETAL.[12]** Alternating current tungsten inert gas (ACTIG) welding was used to create AA6063 aluminium alloy joints, and it was then determined how post-weld heat treatment (PWHT) affected the joints' tensile properties, impact strength, microstructure, microhardness, and fractography. The ACTIG welding method was chosen because it has improved strength, ductility, and lacks any visible microstructure flaws. As-welded (AW) and PWHT samples were created from the welded samples. The samples were subjected to solution treatment (535 °C, 2h), water quenching, and artificial ageing (165°C, 18h) as part of the PWHT procedure. The experimental findings demonstrate that the mechanical and microstructure features of the AA6063 joints after PWHT were much better than those of the AW samples. Impact strength has increased by 22.22% and ultimate tensile strength by 3.72%, respectively.

**ARUNKUMARK,DHAYANITHI GETAL.[13]** This experimental effort involved the use of gas tungsten arc welding with pulsed current at various frequencies (2Hz, 4Hz, and 6Hz) to create weldments in aluminium alloy (5052). The chosen material, an aluminium plate and electrode, is put through a chemical analysis test to ensure that the materials are properly composed. It is put through a weldment with selected settings after achieving successful results. Pulsed welding of two distinct thick materials at various frequencies was compared with non-destructive tests like radiography and liquid penetration tests (2mm and 3mm of 5052 aluminium alloy). This experiment aims to determine how pulsed current affects the weldment quality. The experimental results for different welding parameters for the specified material utilising pulsed and non-pulsed current GTAW are evaluated and compared.

**MR .C. PARTHASARATHY, MR. D. SATHYASEELAN ET AL.[14]** In this experiment, weldments of aluminium alloy (5052) were created utilising gas tungsten arc welding and pulsed current at frequency of 2Hz, 4Hz, and 6Hz. To ensure that the materials are properly composed, the chosen components, an aluminium plate and an electrode, are subjected to a chemical analysis test. It is put through a weldment with the appropriate settings after successful outcomes. Non-destructive testing such as liquid penetration tests and radiography were carried out on

two different thick materials, appraised, and compared with pulsed welding at various frequencies (2mm and 3mm of 5052 aluminium alloy). Investigating how pulsed current impacts the weldment quality is the objective of this experiment. The experimental results for different welding parameters using pulsed and non-pulsed current GTAW for the material in concern are described and compared.

**SEONG MIN HONG, SHINICHI TASHIRO, HEE- SEON BANG ET**

**AL.[15]** The key elements that degrade the joint quality when attaching aluminium alloy to galvanised (GI) steel are the vast differences in thermophysical characteristics, imperfections caused by zinc on the steel surface, and the creation of excessively brittle Fe-Al intermetallics (IMC). In this work, alternating current pulse gas metal arc welding (AC pulse GMAW), which combines electrode positive and negative modes, was proposed as a potential solution. 2 mm diameter AA4047 filler wire was used to link GI steel plates and a 1.2 mm thick AA5052 aluminium alloy. In order to determine the impact of various welding parameters on the development of the Fe-Al intermetallics (IMC) layer, the impact of zinc, and the mechanical properties of the joints, a comparative study on the joint interface was carried out by varying the welding current and electrode-negative (EN) ratio. Polarity changes have been shown to affect how zinc is distributed in joints. With less heat input, a higher EN ratio prevented the IMC layer from growing past 3.59  $\mu$ m. At a welding current of 50 A and an EN ratio of 20, the highest tensile-shear strength of the welded joints was roughly 171 MPa (78% joint efficiency). 20% percentage of EN.

**C.SANJEEV, K.MUTHUKUMAR ET AL.[16]** The automotive, food, and medical equipment sectors now require more welding of heat-sensitive materials, including thin sheets, stainless steel, coated thin plates, mixed welds and aluminium. However, related advancements in the field of arc welding are not well known and are not frequently utilised to the fullest extent. In the context of gas metal arc welding operations, digitization has made it feasible to include software into the source of power, gas control, and wire feeder. It has been suggested to use Gas Metal Arc Welding (GMAW) with pulsed and non-pulsed current at frequencies of 2Hz, 4Hz, and 6Hz to create aluminium alloy weldments.



Welding techniques using pulsed and non-pulsed currents were tested, analysed, and compared to liquid penetration tests, radiography, and various frequencies of thickness materials (2mm of 5052 aluminium alloy). Thus, the method aids in gaining insight into how pulsed current affects the weldment quality. It has been determined that satisfactory process effectiveness can be attained along with good weldability and mechanical joint qualities.

**HASANNIAH, M. MOVAHEDI ET AL. [17]** Al-Mg aluminium alloy was lap bonded to steel sheet covered in aluminium using Al-Si filler metal and pulsed gas tungsten arc welding. Studies of the joint's mechanical properties and microstructure as a result of the welding heat input were done. The creation of intermetallic compounds (IMCs) at the joint interface, the sites of the fractures, and the weld metal microstructure were all examined using stereo, optical, and scanning electron microscopy (SEM) with energy dispersive X-ray spectroscopy (EDS). The shear-tensile test was used to assess the joint strength of the welds. The results showed that the Al-Fe intermetallic thickness was significantly decreased at the weld seam/steel contact to less than 2.5\_μm in the presence of a thin aluminium clad layer with a 350\_μm thickness. The joint strength rose when the heat input was raised up to an optimal level and then began to decline after that. The joint strength achieved 90% of the strength of Al-Mg aluminium base metal at the optimal heat-input of 250 J/mm. In each and every weld, the fracture path showed an angle of 75.3 degrees with respect to the horizontal base plane. Maximum normal stress, not maximum shear or von Mises effective stress, was the main factor determining fracture in the joint, according to a stress study of the weld.

**BALRAMYELAMASETTI, VENKATRAMANAG, VISHNUVARDHANT ET AL. [18]** In this study, the AA5052 and AA6061 weld joints were created utilising the gas tungsten arc welding technique and ER4043 filler. Ultimate tensile strength, hardness, and impact toughness were taken into consideration as output variables together with welding current and root gap parameters. The complete factorial design technique was used to create the studies. For each output response, regression models were created using a linear fit strategy. To further investigate the impact of specific factors on output responses, analysis of variance was carried out. When welding current is 210 A

and root gap is 1 mm, higher tensile strength of 393 MPa and impact strength of 59 J were noted. The primary influencing factors for these dissimilar welded joints are the welding current and root gap.

**BALRAM YELAMASETTI, VENKAT RAMANA G., VISHNU VARDHAN T. ET AL.[19]** Bimetallic welds of AA5052 and AA7075 formed using the gas tungsten arc welding technique were studied for weldability and mechanical behaviour. To link the different metals, two filler wires, ER4043 and ER5356, were used. In both filler weldments, the same welding parameters and conditions were employed. Non-destructive testing was done to verify that the fusion welding procedure could fuse a joint between two different materials. To assess the weld qualities, mechanical testing like tension, hardness, and impact tests were carried out in accordance with ASTM standards. With a UTS of 182 MPa, weldments made with ER4043 filler have shown to be of outstanding quality. It was found that ER 4043 welds had higher impact strength of 62 J, whereas ER 5356's weldments had toughness values of 24 J. When ER5356 filler was used, the weld zone had micro-porous surfaces and voids.

**R. RAMJI, V. BHARATHI, N.R. PRABHU SWAMY ET AL.[20]** Aluminum is a strong, lightweight, and corrosion-resistant material that is widely utilised in the construction, packaging, and transportation industries, among other things. To enhance its qualities, aluminium can be alloyed with substances like silicon and magnesium. Although there are many benefits to welding aluminium alloys, there are occasionally problems with welding aluminium alloys that are related to the alloy content, metallurgy, and method. In the current inquiry, an effort has been made to perform fusion welding for Aluminum 6063 alloys using TIG & MIG procedures. In TIG and MIG welding techniques, many filler rod types and spools of alloy 6061 were employed. Additional characterisation investigations were conducted to evaluate the joints' BHN and tensile strength. To evaluate the various zones and grain formation on the welded connections, microstructure studies were also carried out using metallurgical microscope on TIG and MIG welded joints.

**BALRAM YELAMASETTI, DEEPAK KUMAR, KULDEEP K SAXENA ET AL.[21]** In this study, ER4043 was used as a filler metal during the gas tungsten arc welding

procedure to join the two dissimilar metals, AA5052 and AA7075. Using infrared thermography, the temperature distribution over the weld surface was measured while welding. The residual stresses in each welding pass on various weld zones were measured using the X-ray diffraction technique. According to thermography measurements, passes 1, 2, and 3 had peak temperatures of 712, 789, and 816 °C, respectively. Temperatures were greater in the HAZ of AA5052 than they were at the HAZ of AA7075. Passes 1, 2, and 3 each had a peak residual stress reading of 66, 28 or 45 MPa. There were much lower residual stresses at the HAZ of AA5052 than at the HAZ of AA7075.

### **BALRAMYELAMASETTI, VENKATRAMANA**

**G, SANDEEP MANIKYAM ET AL. [22]** In fusion welding techniques, higher heat input rates and uneven thermal cycles affect HAZ characteristics and lead to the development of residual stress throughout fusion zones. The service life of welded structures is shortened by these heat stresses. In-Situ peak temperatures and their distribution over the weld surface of similar and dissimilar combinations of Monel 400 and AISI 316 base plates joined by constant and pulsed current TIG welding processes are measured with infrared thermography technique at various time intervals to better understand the thermal cycles. After the joints were welded, the X-ray diffraction technique was used to measure the thermal stresses that had accumulated across the joints. On both sides of the base metals, the weld surfaces of the fusion zone and HAZ were measured for stress. The constant welding approach recorded higher temperature values than the pulsed welding technique. Additionally, weldments made using a continuous welding process were more impacted by heat. During passes 1, 2, and 3 of the CCGTAW process, the highest temperatures were 1657 °C, 1711 °C, and 1748 °C, respectively. While during pass-1, pass-2, and pass-3 welding in the PCGTAW process, high temperatures of 1434 °C, 1509 °C, and 1634 °C, respectively, were measured. The 10.6% overall temperature decrease in the PCGTAW process may have an impact on the cooling cycles during solidification. In joints with different compositions, both welding processes have shown the generation of residual stresses of a compressive nature. Lower residual strains were produced as a result of the pulsed technique's reduction in the heat concentration at the fusing region

**V. SANDHYA, ALMAS SADAF, B. POOJA REDDY ET AL.[23]** The weld bead properties are significantly influenced by process parameters. The purpose of this research is to investigate how different characteristics, such as gas flow rate, voltage, and current, affect the weld that is produced. For the trials, TIG welding of aluminium 6063 and 7075 was done using the Taguchi design. For each specimen, the defects and the weld bead mechanical characteristics are examined. Voltage is the aspect that has the largest influence, according to the findings.

**ZHAOYANG YAN, TAO YUAN & SHUJUN CHEN ET AL.[24]** The grain size of regular welds and those welded at various oscillation frequencies were used to study and debate the mechanism of the microstructure refinement of metals and alloys (5052 and 6061) by arc oscillating. Fine columnar crystals started to form in the 5052 alloy around the "internal fusion line" during oscillating arc welding, and the oscillating arc with low and high frequency significantly refined the grains. The grain refinement of 6061 Al alloy during arc oscillation welding was, however, limited because of the specific crystal growth pattern at the fusion line and the properties of the material. It is brought on by different material qualities rather than a change in the method for refining grains.

**SKATO,STANABE ET AL.[25]**The impact of pulsed TIG welding's control over heat input is significant. Compared to DC TIG welding, the current range where acceptable beads can be created is wider, and by choosing the right pulse circumstances, good, narrow bead shapes can be achieved. The choice of shielding gas during pulsed TIG welding drastically affects the results. The following variations between He and He+Ar gas were shown. Based on the foregoing findings, it is believed that pulsed TIG welding with He gas can produce high-quality welds when welding aluminium alloy sheets at high speeds and with thicknesses greater than 1 mm.

**P.K. MINIAPPAN, V.V. ARUN SHANKAR, A. SAIYATH IBRAHIM ET AL.[26]** Gas tungsten arc welding is the most widely used welding method for joining aluminium and aluminium alloys (GTAW). It makes it possible to get clean, defect-free welds and to the degree of removing the oxide layer that has built up on it. The numerous

types of welding power supplies (DCEP/DCEN/AC) that can be utilised, the welding speed, and the various shielding gases that can be employed all have an impact on the weld joint. The accuracy and effectiveness of the welding are determined by these variables. This paper examined the different factors that affect weld quality as well as how welding variables like power supply, welding speed, and shielding gas affect the weldment mechanical properties. The current study examines the impact of welding parameters on the weldability of 5052 aluminium alloy, including welding speed, power supply type, and shielding gas type. For superior weld results, a systematic methodology (Taguchi method) has been used. The weld quality has been optimised in relation to the appropriate welding parameters using software called Minitab.

**W.B. CHEN ET AL.[27]** To weld 5052 Al alloy to Ti-6Al-4V alloy in a butt configuration, a tungsten inert gas welding-brazing process utilising filler metal with an aluminium foundation has been devised. According to the findings, heat input had an impact on the Al/Ti joints' interfacial reaction layer's morphology and thickness, which had an impact on the weldment's mechanical characteristics. Thin cellular-shaped and club-shaped TiAl reaction layers occurred in the brazing zone with a welding current of 70 A and an optimised tungsten electrode offset D of 1.0 mm, which assisted in preventing fracture formation and propagation during tensile testing, from the original Al/Ti contact to the Al side. The optimised Al/Ti joint eventually shattered at the base plate of the Al alloy, reaching a maximum tensile strength of 183 MPa. Additionally, the Al/Ti joints' joining process and power density characterization were examined.

**A. RAVEENDRA, B. V. R. RAVI KUMAR ET AL.[28]** In this experiment, gas tungsten arc welding was used to produce weldments of the aluminium alloy (5052) at varying frequencies of 2Hz, 4Hz, and 6Hz using pulsed current and non-pulsed current. Pulsed and non-pulsed current welding of two distinct thick materials at various frequencies was conducted, analysed, and compared with non-destructive tests like radiography and liquid penetrant testing (1.5mm and 2.5mm of 5052 aluminium alloy). This experiment aims to determine how pulsed current affects the weldment quality. The experimental results for different welding parameters for the mentioned material utilising pulsed and non-pulsed current GTAW are investigated

and evaluated.

**T. E. ABIOYE, H. ZUHAILAWATI, S. AIZAD ET AL.[29]** To find the ideal combination of laser pulse current, pulse frequency, and pulse length that satisfies the AWS D17.1 criteria for the aerospace industry, pulse laser welding of 0.6 mm-thick AA5052-H32 was conducted. Additionally, the weldments mechanical characteristics and microstructure were examined. Weld bead geometry and the parameters were discovered to be related. At (I) Low average peak power (17.6 J), low pulse energy (17.6 J), and high-quality weld joints that do not even break due to solidification comply with AWS D17.1, and (II) High average peak power (4.2 kW) and high pulse energy (25 J) standards were obtained (2.8 kW). The dendritic grain structure of the weld joint with reduced heat energy input was finer. The hard phase compound (Al<sub>0.5</sub>Fe<sub>3</sub>Si) production and magnesium vapourization were reduced in the weld joint created with less heat energy input. When compared to the weldment generated at higher heat energy input, the tensile strength of the lower heat energy input weldment (168 MPa) is 1.15 times higher, although it showed a 29% loss in hardness (111 HV<sub>0.10.5</sub>) at the junction. To achieve AWS D17.1-compliant 0.6 mm-thick AA5052-H32 pulse laser weld junctions criteria for aviation structures, it is essential to choose the right parameters.

**SHARDA PRATAP SHRIVAS, SANJAY KUMAR VAIDYA, ASHISH KUMAR KHANDELWAL ET AL.[30]** There are many different welding techniques, but tungsten inert gas (TIG) welding is particularly important for joining thin sections of non-ferrous metals such stainless steel, copper alloys, aluminium alloys, and magnesium. TIG welding has many benefits when combining dissimilar metals, including the reduction of heat- affected zones and the avoidance of slag. Since input parameters significantly impact the calibre of a welded specimen. To construct the experiment, collect the data, and increase the tensile strength of variation in welding conditions, an experimentation strategy based on a L<sub>9</sub> orthogonal array was adopted. In the end, experiments were conducted to determine the ideal process parameters for the chosen aluminium alloy, and their success was confirmed by SEM in the analysis of strength.

**ZHENG YE, JIHUA HUANG ,WEI GAO ET AL.[31]** The final qualities of the Al/steel butt joint produced by conventional techniques are significantly impacted by unstable weld appearance and unpredictable interfacial compounds. The MIG-TIG double-sided arc welding-brazing (DSAWB) method was employed in this study to butt-join Q235 low-carbon steel and AA5052 aluminium alloy. Research was done in-depth on the joints' mechanical characteristics and microstructure in contrast to the typical metal inert gas (MIG) joint. The results showed that excellent weld appearance, particularly back appearance, was generated at a welding heat input less than that in the conventional MIG method because to the double-sided heating and gas shielding in the DSAWB method. At the brazing interface, needle-like FeAl<sub>3</sub>, lamellar Fe<sub>2</sub>Al<sub>5</sub> heat input, and the maximum thickness of the FeAl<sub>5</sub> were observed. As a result of the reduced 2Al<sub>5</sub>, the effective limit was 2.03 m. However, when the ideal settings were used, enormous FeAl<sub>3</sub> and Fe<sub>2</sub>Al<sub>5</sub> layers measuring 4.20 m thick with evident fissures were discovered in the conventional MIG. The DSAWB joints average tensile strength was 148.1Mpa, 2.5 times more than that of the conventional MIG joints. This achievement was made possible by the superb weld appearance and the successful management of the interfacial intermetallic compound.

**C Y SONG, Y W PARK, H R KIM ET AL.[32]** The purpose of this study is to determine the ideal laser hybrid welding settings for a 5052- H32 aluminium alloy. Using the technique of non-linear transient thermal analysis, the thermophysical phenomena in the welding process are simulated. To determine the ideal welding settings that minimise residual stress and strain, Taguchi's parameter design method is used. The findings of the experiment are compared to those achieved by design of experiments (DOE) and Taguchi's parameter design using welding simulations. Approximation models like the radial basis function neural network and the polynomial- based response surface technique are built using DOE data. These approximation models make it simple to estimate, in accordance with parameter variations, the relationship between welding parameters and thermo-mechanical responses.

**PRATIK KIKANI ET AL.[33]** Trolley is the name for the platform that an automobile engine is mounted on. A trolley is a particular sort of structure in which



MIG welding is used to join various support components, such as the main channel, support channel, shaft-bar, hook angle, handle, etc. The trolley is comprised of two metal parts, mild steel and hot rolled steel, and can hold 18 kg of engine weight (i.e. MS, HR). The paper examines the effects of several process factors, including current, voltage, welding speed, electrode material, and various mechanical characteristics, including hardness, tensile strength, and compressive strength. Comparison results are shown by modifying the relevant process parameter data.

**SHANAVASS, EDWINRAJADHASJETAL.[34]** The strongest non-heat treatable aluminium alloy is from the 5xxx series of aluminium alloys. It is employed in automotive parts and structure of the body due to its outstanding high corrosion resistance, formability, weight savings, and strong strength. In the current work, the effect of TIG welding parameters on the quality of the weld on plates made of the AA5052 H32 aluminium alloy was investigated, and the mechanical characteristics of the resultant joint were compared to those of a Friction Stir (FS) welded connection. The welding current and inert gas flow rate are the selected input variable parameters. Based on the results of multiple test runs, other variables including welding speed and arc voltage were maintained throughout the study. The weld's quality is determined by using ultimate tensile strength. To ensure that TIG welded joints are as strong as possible, double pass V-butt joints were created on one side. Both the macro and microstructural examination of the welding processes were done.

**M.SHUNMUGASUNDARAM, A.PRAVEENKUMAR, L.PONRAJSANKARETA L.[35]** Friction stir welding is a non-consumable material state welding process used in the aerospace, railway, automotive, and nautical industries to join dissimilar aluminium alloys. The process parameters, such as the tool's rotational speed, the welding speed, and the tilt angle, affect the welding quality of this form of friction stir welding. Friction stir welding is used to join plates made of the dissimilar aluminium alloys AA6063 and AA5052, and Taguchi L9 orthogonal design of experiments is used to improve the process parameters. To improve the tensile strength of the weld joint, the best process variables are identified. ANOVA is used to examine the appropriate range of process factors and their effects on the strength of the weld joints. The friction stir welding technique successfully joins the sheets, and



to evaluate their strength, the welded sheets perform a tension test at room temperature. The outcome demonstrates that the welding speed has a greater impact on joining these different connections than the feed and tilt angle.

**ARIOSUNARBASKORO, MOHAMMADAZWARAMAT ET AL. [36]** In tungsten inert gas (TIG) welding, this work describes an automated or intermittent wire feeding technique. Using one combination proportion of filler metal and several welding parameters, the preliminary experiment demonstrates the effects of macrostructure, microstructure, and mechanical property on various welding parameters. Microstructural analysis of the weld metal with high-density eutectic phase revealed localised segregation at the centre area, and energy dispersive X-ray spectroscopy (EDS) analysis revealed that Mg content was higher there than elsewhere. Other sample microstructure demonstrates the formation of columnar structure at dilution boundaries and indicates that the filler wire's insertion was followed by rapid cooling. Additionally, the microstructure of the weld traverse section demonstrates how the heat input affected the wavy structure. The fracture mode demonstrates that oxidation is susceptible to a lack of heat input, leading to the tendency for fracture to occur at the weld metal in a brittle way with a greater than 40% reduction in strength. The length ratio (R) and volume ratio (RV) calculation methods were also described in this article in order to estimate the minimum ratio value under the assumption of a satisfactory welded surface profile.

**AMIR HADADZADEH, MAJID MAHMOUDI GHAZNAVI ET AL. [37]** Investigations were made on the heat affected zone (HAZ) softening behaviour of the gas tungsten arc welding (GTAW)-welded strain-hardened Al-6.7Mg alloy. Wider HAZs were created as a result of welding with more heat input. In addition, larger heat inputs resulted in larger precipitates. As a result, by increasing the heat input, the welding joints' strength was decreased. In order to increase the strength of the joints, the pulsed-GTAW (PGTAW) method was used in the second phase of the investigation. The fracture during the tensile test was found to have shifted from the HAZ to the fusion zone, improving the overall strength of the welding joints. The impact of duration ratio and pulse frequency was also studied. In the current investigation, the duration ratio had no significant influence on the

welds strength and microstructure, while raising the frequency made the welds strength and microstructure finer.

**G. MADHUSUDHAN REDDY, A. A. GOKHALE, K. PRASAD RAO ET AL.[38]** In sheets of the AA8090 type of aluminium lithium alloy, the effects of pulsation frequency of current on weld bead hardness, microstructure, and tensile properties were investigated. It was noted that the standard (i.e., continuous current) gas tungsten arc welding procedure resulted in a primarily columnar structure in the as-solidified weld. The addition of current pulsing caused the grain structure to become finer and more evenly distributed. Additionally, there was a preferred frequency range where grain refining was at its highest. Maximum hardness, maximum ultimate tensile strength, and maximum % elongation all fell within the same optimal frequency range. Typically, tensile strength enhanced with solution treatment and ageing (STA). Welds deposited with a 6 Hz pulse frequency in the STA condition had the best tensile property combination.

**RAJESH P VERMA, YOGESH SHARMA ET AL.[39]** This research investigates how the filler metal affects the mechanical and microstructural properties of two dissimilar aluminium alloys, 5083-O and 6061-T6, when they are welded together using metal inert gas. Because aluminium alloys are frequently joined using metal inert gas welding, it was chosen for usage in a variety of important commercial applications, including aerospace, marine, automotive, and many others. ER4043 and ER5356 were used as filler metals in the construction of the joints. To determine the tensile strength, both welded samples were cut in accordance with ASTM B-557M, and Vickers hardness measurements were made at the base metal, heat-affected zone, and welded metal. Optical micrographs were used to analyse the mechanical characteristics of welded samples. According to the findings, filler metal ER5356 was better able to improve the mechanical properties and characteristics of the welded samples microstructure.

**P. PRAVEEN, P.K.D.V. YARLAGADDA ET AL.[40]** The aim of more recent

automobile designs is weight reduction. This need has led to some intriguing advancements in the light metal industry. A conventional light metal used in manufacturing is aluminium. Manufacturers are faced with newer difficulties as the use of aluminium as an alternate material increases. Development of novel aluminium alloys, joining of various types of aluminium alloys, and enhancement of weld quality of welds and weld repairs are some of these new difficulties. Pulse gas metal arc welding is one of the methods that aluminium fabricators are investigating (GMAW-P). This study examines the issues associated with connecting newer types of aluminium alloys and how GMAW-P can help in overcoming these challenges.

**RAVENDRA, A. ET. AL [41]**The purpose of this study is to determine how the Gas Tungsten Arc Welding process parameters impact the depth of penetration of a particular specimen. In this study, the effects of TIG welding parameters on the weldability of specimens made of 5052 aluminium alloy with dimensions of 100mm long, 50mm broad, and 2.5mm thick are investigated. Welding variables such as arc voltage, welding current, welding speed, gas flow rate, and heat input affect the depth of penetration measured after welding.

**ZHILI FENG ET. AL. [42]**This work shows the results of the mechanical driving force (mechanical strain evolutions) in the temperature range of solidification brittleness where solidification cracking occurs. Autogenous gas tungsten arc welding (GTAW) is simulated due to its frequent use in weldability studies. The FEA models are focused on full penetration bead-on-plate welding on thin plates made of the aluminium alloys 2024-T4 and 5052-0. The commercial general-purpose FEA code ABAQUS is utilised in this work.

**AKASH CHAND, SUNIL KUMAR YADAV ET. AL. [43]**TIG welding is one of the most often used joining techniques for aluminium alloys. This method of arc welding is chosen over others because it yields a good weld bead and needs less metallurgical modification outside the HAZ to achieve good mechanical characteristics. Process variables such as welding speed, current, voltage, and gas flow rate played a major role in determining the accuracy and quality of the weld joint. This research concentrated on TIG welding process parameters such as (travel speed,

and current) with an emphasis on the study and improvement of mechanical properties of weld joints and process parameter optimization. Throughout the investigation and process parameter optimization, other factors remained constant.

**RAVEENDRA A, DR.B.V.R.RAVI KUMAR, DR.A.SIVAKUMAR AND V.PRUTHVI KUMAR REDDY ET. AL [44]** Welding parameters are crucial for joining the work components while TIG welding 5052 aluminium alloy. This study discusses the impact of welding parameters on the weld bead shape, such as front and rear weld joint width. It was found that increasing the welding current led to an increase in heat energy on the work piece surface as well as a linear increase in the front and back widths of the weld joint during the experimental work. The welding current, gas flow rate, and welding speed were all taken into consideration. The front and rear widths of the weld connection linearly shrink as welding speed increases.

**A. RAVEENDRA, B. V. R. RAVI KUMAR & S. SUDHAKARA REDDY ET. AL. [45]** A metal's hardness refers to its capacity to withstand penetration. Changes in metallurgy are brought about by welding. These transitions are described by the hardness measurement. Weldment micro hardness will be thoroughly investigated in order to increase the mechanical durability of welds. The current study examined the mechanical and microhardness characteristics of weldments made of the 5052 aluminum alloy using nonpulsed and pulsed current welding at frequencies of 2, 4, and 6 Hz.

**A. KUMAR & S. SUNDARRAJAN ET. AL. [46]** The current work focuses on enhancing the mechanical properties of AA 5456 Aluminium alloy welds utilising a pulsed tungsten inert gas (TIG) welding technique. By adjusting the pulsed TIG welding process parameters, the Taguchi technique was employed to enhance the mechanical qualities of welds made from the AA 5456 Aluminium alloy. There are regression models available. Analysis of variance was used to see whether the models that were generated were appropriate. Investigations on how planishing affected mechanical attributes revealed an improvement in those aspects. The microstructures of each weld were investigated and related to their mechanical properties.

**TAPAS BAJPEI, H. CHELLADURAI AND MOHD. ZAHID ANSARI [47]** In this

work, transient temperature and residual stresses in different aluminium alloys welded with gas metal arc welding (GMAW) (AA) are to be determined. A moving heat source model based on Goldak's double ellipsoid heat flux distribution is utilised in finite element simulation of the welding process. The three-dimensional thermal and mechanical equations were resolved using the ANSYS Workbench software. Element death and birth code was developed to model the amount of material added during the investigation. The effects of conduction, convection, and radiation were considered in transient thermal analysis. Temperature-dependent variables included in the welding simulations were thermal conductivity, heat capacity, yield stress, elastic modulus, and thermal expansion. The results showed that the AA 6061-T6 plate produced lower temperatures.

**ANKUR DUTT SHARMA AND RAKESH KUMAR SHARMA ET. AL[48]**The popularity of aluminium and aluminium alloys has grown recently. These have excellent corrosion resistance, malleability, formability, and electrical and thermal conductivity. Due to gases dissolved during the melting process, high machinability and workability aluminium alloys are more prone to porosity. Since the technology's development in 1991, aluminium alloys have been the subject of this investigation. Along with discussing the usage of aluminium alloys and the material thicknesses used in various processes, the principles of FSW are also covered.

**M OKUBO & K TAKENAKA ET. AL [49]**In this study, the weldability of A5052 wrought alloy and AC7A castings in gas tungsten arc and electron beam welding was examined. The scientists conducted impact testing, hardness tests, and microscopic investigations. In electron beam welding, the tensile and impact properties of the wrought alloy weld metal and heat affected zone are satisfactory. While the AC7A HAZ has micro-liquidation cracks, the weld metal has micro-solidification fissures.

### **3.2 Literature summary:**

- Employing pulsed current for the GTAW process reduces the heat input and the overall strength of the joint increases.
  
- No defect was observed on the weldments with non-

pulsed current and pulsed current weldments during the liquid Penetrant test.

- For better strength and cleanliness in TIG welding of aluminum, AC power source is mostly preferred.
- The selection of the shielding gas in pulsed TIG welding has a major influence on the result.
- There is a major research report in FSW.
- However, GTAW and PCGTAW have the potential to join aluminum alloy.

### **3.3 Problem identification:**

- Choosing the correct filler material is critical when welding dissimilar aluminum alloys.
- Welding dissimilar materials requires careful adjustment welding parameters to ensure the proper heat input and avoid thermal damage to the weaker material.
- Dissimilar materials may require different preparation techniques due to their different properties.
- Aluminum alloy AA5052 and AA6063 dissimilar metals are challenging material to be weld.

### **3.4 Research objective:**

- To investigate the influence welding process parameter for tensile & hardness.
- To carry out design of experiment with selected process parameters using central composite design.
- To perform tensile & hardness test on welded samples.
- To optimize process parameter using response surface method.

- To validate optimized process parameters with confirmation test

## CHAPTER -4

### METHODOLOGY

---

#### 4.1 Flow of Entire work

The steps taken during the complete project study which is mention below:

1. Identification of material and its grade should be carried out in order to determine the materials suitability for welding.
2. For a good mechanical property, choose input and output process parameters carefully, and optimize this input parameter.
3. Create a Design of Experiments (DOE) for the input parameter optimization using the Full Factorial Method.
4. Carry out the experiment using the input parameter values which had chosen.
5. Conduct the liquid penetrant test for inspect the weld defect in welded specimens.
6. Inspection and tensile strength testing of experimental samples, as well as hardness testing of the weldment sample.
7. Regression analysis is used to generate mathematical equations for the Full Factorial model.
8. To acquire a better outcome, optimize the input parameters and compute the values of the output parameters for the same.
9. Test the tensile strength and hardness of the weldment by performing a sample weld with the optimum input parameters.
10. DESIGN EXPERT software can be used to compare and validate results.



## 4.2 Parameters Selection for project work

- **Input parameters**
  - Peak current
  - Base current
  - Pulse per second
- **Output parameters**
  - Tensile strength
  - Hardness

## 4.3 Range of parameters:

**Table 4.1 Range of parameters**

<b>Parameter</b>	<b>Level-1</b>	<b>Level-2</b>	<b>Level-3</b>
Peak current (A)	160	180	200
Base current (A)	80	90	100
Pulse per second (Hz)	110	130	150

## CHAPTER –5

### DESIGN OF EXPERIMENT

#### 5.1 Experimental Design:<sup>[8]</sup>

Experimental Design (ED) or Design of Experiments (DOE) is a step in the SPC (Statistical Process Control) process, respectively. To achieve the best results, various experimental designs are used in this process. These experimental designs can be quantitatively illustrated in order to optimize the parameter.<sup>[8]</sup>

#### 5.2 Central composite design (CCD):<sup>[8]</sup>

A particular type of response surface design called central composite design (CCD) is used in studies to find the best values for numerous independent variables, or components. The factor levels, the axial points, and the centre point are the three different kinds of experimental variables used in CCD.

The central composite design consists of two phases:

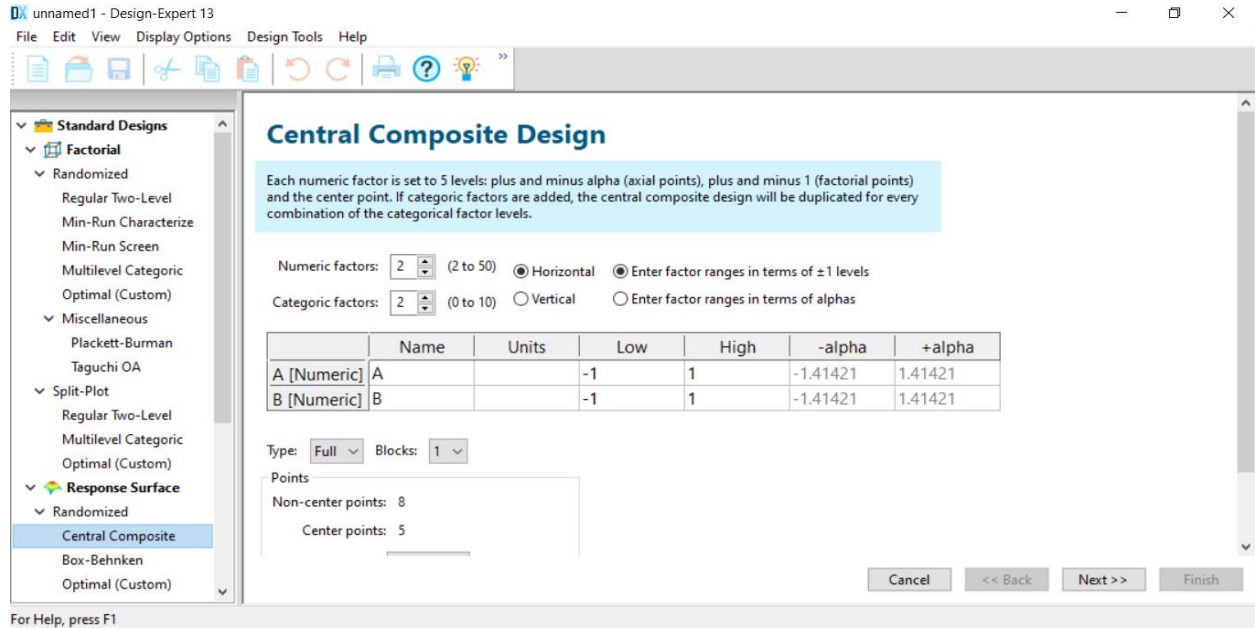
- The first stage involves conducting a number of experiments at various levels of specified factors. These levels are often selected using methods of statistics such as factorial or fractional factorial designs, or based on prior understanding of the system.
- Additional tests are conducted at a series of axial locations that are spaced a certain amount from the centre point during the second phase. These axial locations are intended to record any response surface curvature.

In order to evaluate experimental error and to give a baseline response value for comparison with the responses obtained at the other experimental locations, the centre point is often repeated several times.

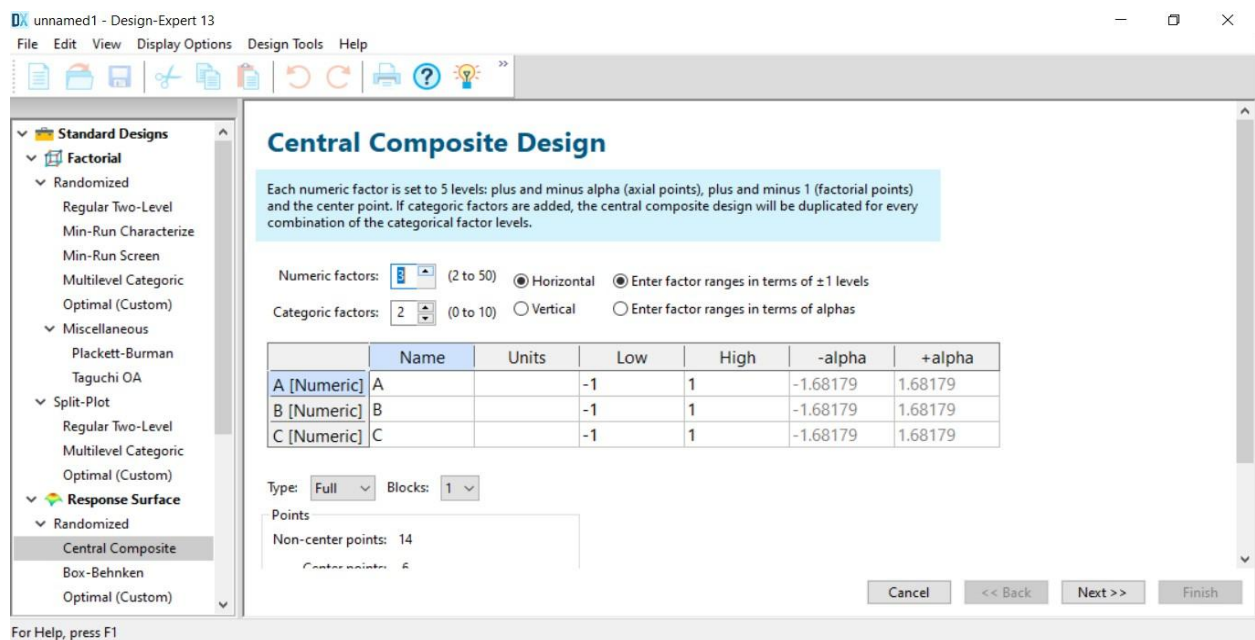
To find the most effective settings for the parameters that optimise the desired result, the response values acquired from the experiments are evaluated using statistical models, such as regression analysis or ANOVA. The analysis' findings could also provide insight regarding how the various variables interact and affect the response.

CCD is frequently used in engineering, chemistry, and other fields where an outcome of interest is affected by a number of parameters, and where the response is to be optimized by determining the ideal setting for each factor.

### Step 1. Select standard design/Response surface/Randomized/Central composite



### Step 2. Select numeric factors



### Step 3. Select number of factors ‘3’

unnamed1 - Design-Expert 13

File Edit View Display Options Design Tools Help

**Central Composite Design**

Each numeric factor is set to 5 levels: plus and minus alpha (axial points), plus and minus 1 (factorial points) and the center point. If categorical factors are added, the central composite design will be duplicated for every combination of the categorical factor levels.

Numeric factors: 3 (2 to 50)  Horizontal  Enter factor ranges in terms of  $\pm 1$  levels

Categorical factors: 0 (0 to 10)  Vertical  Enter factor ranges in terms of alphas

	Name	Units	Low	High	-alpha	+alpha
A [Numeric]	Peak Current	Amp	160	200	160	200
B [Numeric]	Base Current	Amp	80	100	80	100
C [Numeric]	Pulse Per Sec	Hz	110	150	110	150

Type: Full Blocks: 1

Points

Non-center points: 14

Center points: 5

Cancel << Back Next >> Finish

For Help, press F1

### Step 4. Select input parameter and their value

unnamed1 - Design-Expert 13

File Edit View Display Options Design Tools Help

combination of the categorical factor levels.

Numeric factors: 3 (2 to 50)  Horizontal  Enter factor ranges in terms of  $\pm 1$  levels

Categorical factors: 0 (0 to 10)  Vertical  Enter factor ranges in terms of alphas

	Name	Units	Low	High	-alpha	+alpha
A [Numeric]	Peak Current	Amp	160	200	160	200
B [Numeric]	Base Current	Amp	80	100	80	100
C [Numeric]	Pulse Per Sec	Hz	110	150	110	150

Type: Full Blocks: 1

Points

Non-center points: 14

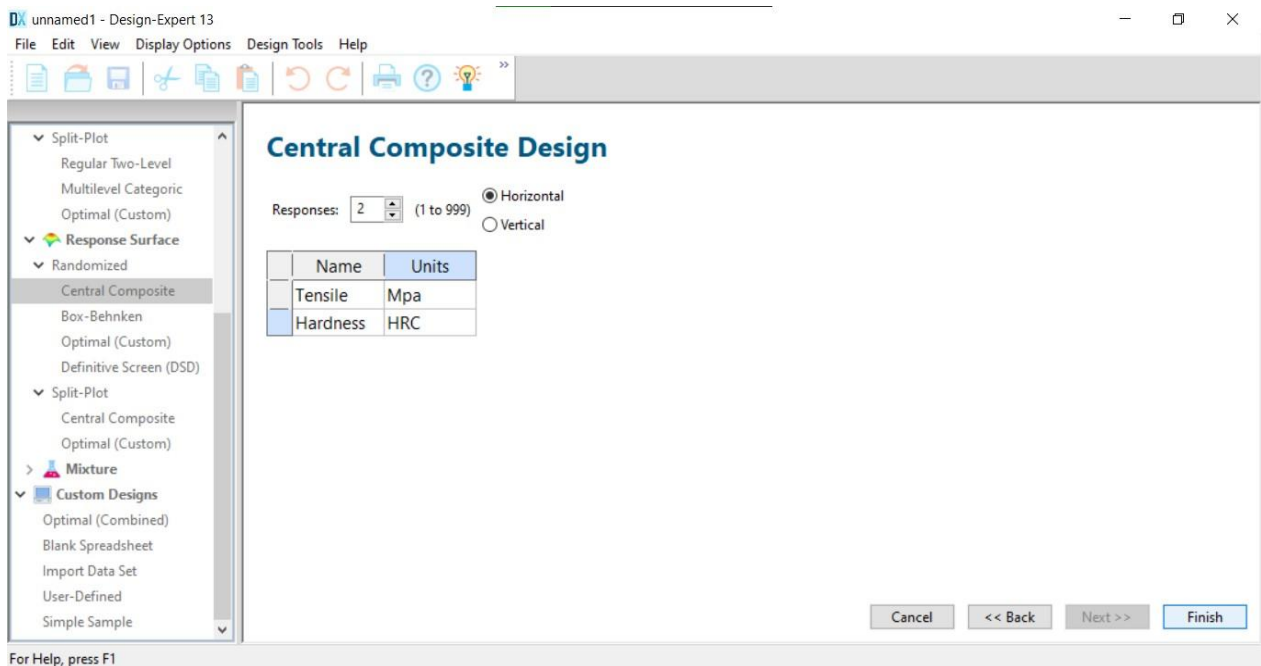
Center points: 6

alpha = 1 Options... 20 Runs

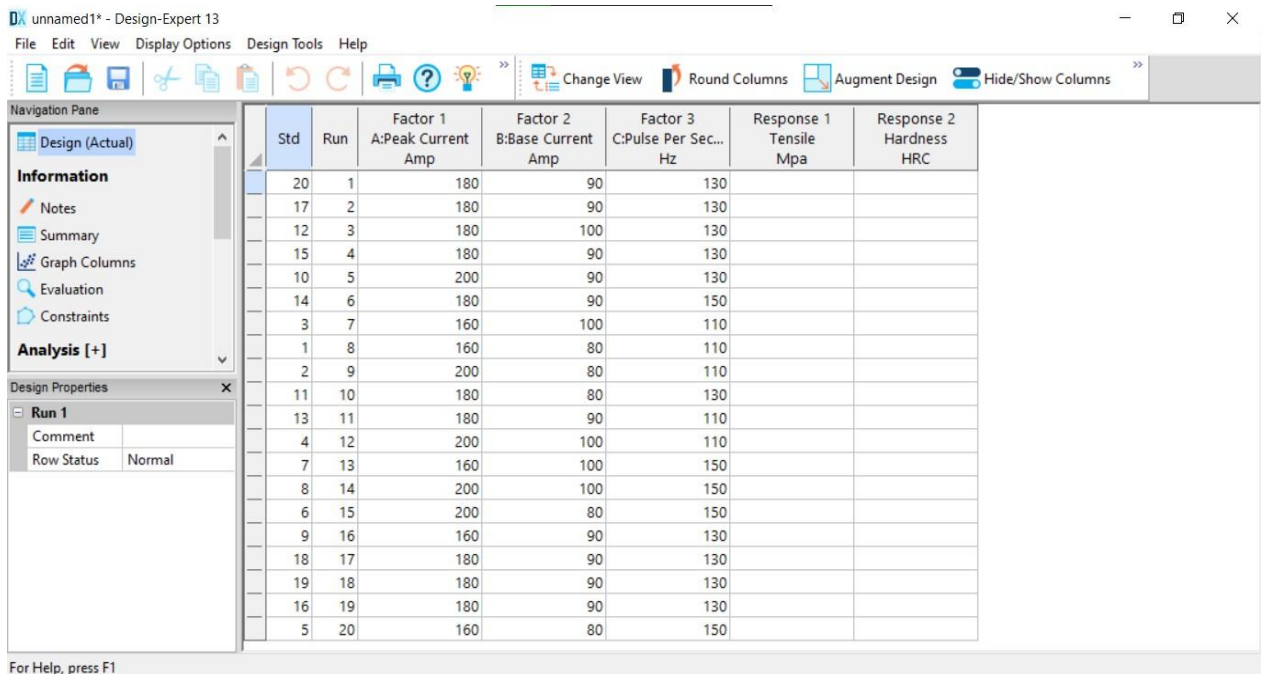
Cancel << Back Next >> Finish

For Help, press F1

### Step 5. Select responses '2'/Output parameters



### Step 6. D.O.E. for response surface method



**5.3 Design of Experiments(D.O.E)**

<b>Ex. No.</b>	<b>PeakCurre nt</b>	<b>BaseCurrent</b>	<b>PulsePerSeco nd</b>
1	160	80	110
2	160	80	150
3	160	90	130
4	160	100	110
5	160	100	150
6	180	80	130
7	180	90	110
8	180	90	130
9	180	90	130
10	180	90	130
11	180	90	130
12	180	90	130
13	180	90	130
14	180	90	150
15	180	100	130
16	200	80	110
17	200	80	150
18	200	90	130
19	200	100	110
20	200	100	150

**Table 5.1 Experiment combination from design expert software**



## CHAPTER - 6

### EXPERIMENTAL WORK

#### 6.1 Apparatus

##### 6.1.1 Base material

The experimentation occurred on two different aluminum alloys, AA5052 and AA6063. Table 2.4 indicates its mechanical properties and chemical composition.



**Fig.1 BasemetalAA6063 aluminumalloy**

The above fig. 6.1 shows the base metal of AA6063 aluminum alloy



**Fig.2 BasemetalAA5052 aluminumalloy**

The above Fig. 6.2 shows the base metal of AA5052 aluminum alloy

## 6.2 Consumable and electrode

Solid rod of the ER4043 type, measuring 1 meter in length, is the consumable used in welding. Tungsten zirconium coated 2mm electrodes are used in the welding process.



**Fig 6.3ER4043 FillerWire**

- This TIG welding procedure uses a separate welding rod as the filler metal to melt and combine the metals, thus the electrode is not consumed during welding.
- It is 99% tungsten in composition.
- This electrode's benefits include simple striking and arc stability, a high allowed current density, and a decreased chance of tungsten inclusions.

## 6.3 Joint design of weld

Weld axis length : 200

Root gap R : 2 mm

Root Face F : 2mm

Included Angle: 60

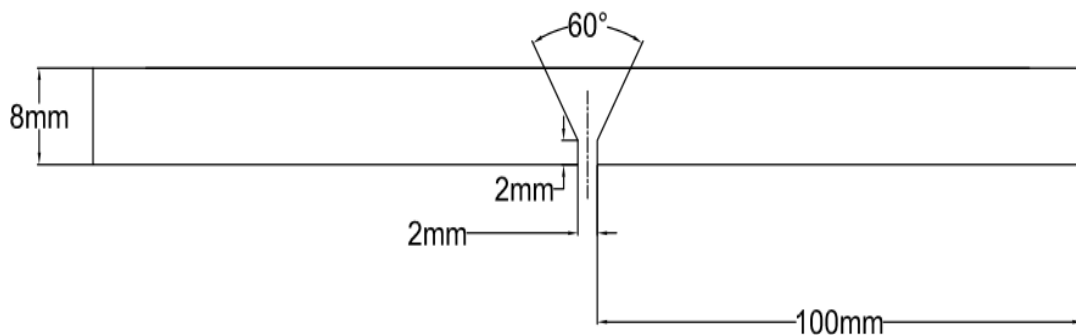


**Fig 6.4Joint design**



## 6.4 Edge preparation

The experiment uses a 8 mm thickness AA5052 and AA6063 dissimilar aluminum alloy plates. The weld edge preparation on the grinding equipment is shown in Fig. 6.5.

With the use of a grinding machine, a 60° angle 'V' groove was created on the base material.



**Fig6.5 edgepreparation on Hand Grinder**



**Fig6.6Includedangle60°**

## 6.5 Performing experiment

The TIG welding setup for welding the test piece is shown in below Fig. 6.7.



**Fig 6.7 TIG welding machine setup**



**Fig 6.8 Performing welding experiment**

## 6.6 Welded Specimens

Figure 6.9 below demonstrates how the specimen was welded in accordance with the run order determined by the Design expert software. A total of 20 specimens were prepared for the experimental investigation.



**Fig 6.9**Welded specimens

## 6.7 Liquid Penetrant Test<sup>[9]</sup>

A nondestructive testing technique called liquid penetrant testing (LPT) is used to find surface-breaking defects in materials. The technique relies on the capillary action theory and involves applying a liquid penetrant to the material's surface, allowing and allowing it to soak into any surface-breaking cracks. Following the removal of the penetrant from the surface, the area is treated with a developer to draw the penetrant from the imperfection and make it visible.

In general, this procedure is a low-cost testing method for identifying flaws in the industry, such as surface cracks in casting parts, welding joints, and forging components.

The DP test process is described in ASME section X (Non-destructive testing), specifically for detecting surface flaws.



## 6.7.1 Inspection steps for Liquid Penetrant Test<sup>[9]</sup>

### 6.7.1.1 Pre-cleaning:

In order to identify faults, the test surface must first be free of any debris, including dust, oil, grease, and other materials that may have been present on the surface of the work being tested. Depending on the application, you can clean the surface using a cotton cloth, solvents, or even an alkaline solution.

### 6.7.1.2 Penetrant application:

Once the surface has undergone pre-cleaning, penetrant are applied to look for surface flaws. An oily luminous liquid called Penetrant. Low surface tension and capillary action in Penetrant make it ideal for spotting flaws. The dwell duration varies depending on the type of material being examined, but it typically ranges from 5 to 30 minutes. Figure 6.13 demonstrates the need for applying penetration.

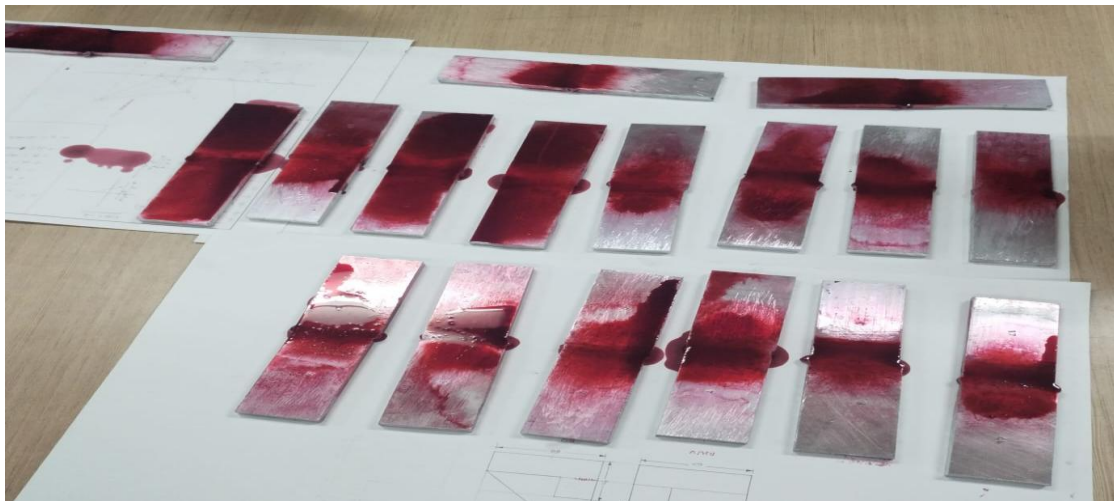


**Fig 6.10 Application of penetrant on specimen<sup>[9]</sup>**

### 6.7.1.3 Excess Penetrant Removal:

Excess penetrant was cleaned from the job's surface when the dwell time was finished. The cleaning technique was dependant on the sort of penetration employed.

For surface cleaning purposes, water-washable solvent is typically utilised in all industries. Keep in mind that you shouldn't apply the cleaner to the job's test surface.

**6.7.1.4 Developer application:**

After the excess penetrant was removed, the white developer is applied on the surface of the job. There are many developers available in the market like an aqueous wet developer, dry powder, water-soluble, and also water-soluble respectively. If the defect was present on the surface that was known as "bleedout". Fig.6.14 shows that we have to apply developer on the surface.



**Fig 6.11 Application of developer on specimen<sup>[9]</sup>**

**6.7.1.5 Inspection:**

The inspector will test for flaws using visible light. The inspection period is typically 10 to 30 minutes after the developer has been applied to the surface of the job, depending on the developer and penetrant employed.

**6.7.1.6 Post - cleaning:**

The surface has been carefully cleaned after the inspection and recording have been completed. The post-inspection coating procedure is then scheduled in accordance with the needs of the customer.

**6.7.2 Advantages:**

- Surface-breaking faults that are so minute they might not be visible to the human eye can be found using LPT. Due to its high sensitivity, it can be used to detect fractures, porosity, laps, and seams.
- In comparison to other methods like radiography or ultrasonic testing, LPT is a nondestructive testing technique that is reasonably inexpensive. The tools and supplies needed for LPT are easily accessible and reasonably priced.
- A variety of materials, including metals, polymers, ceramics, and composites, can be treated with LPT. Both ferrous and non-ferrous materials can be utilized with it.
- LPT is a relatively straightforward nondestructive testing technique that needs little training or experience. The technique can be used on-site, which makes it a practical and effective way to evaluate materials.
- LPT is a nondestructive testing technique that doesn't subject workers to radiation or other dangerous substances. It is a way of testing that is both secure and kind to the environment.
- Surface-breaking imperfections are visible with LPT, making it simple to find and locate any flaws.

### **6.7.3 Disadvantages:**

- LPT can only identify surface-breaking flaws, which means it might not be able to identify internal or subsurface issues. The procedure necessitates direct access to the surface being evaluated, which can be difficult for places with restricted access or complex shapes.
- Human error can reduce LPT's efficacy by affecting how the penetrant or developer is applied, how thoroughly the surface is cleaned, or how accurately the results are interpreted.
- LPT is a time-consuming procedure that includes several processes, including cleaning, penetrant application, penetrant excess removal, and developer application. As a result, it may be slower than other nondestructive testing methods like radiography or ultrasonic testing.
- Some penetrant types used in LPT may need special handling and disposal techniques since they may be environmentally hazardous.
- LPT may not be able to detect deeper flaws or imperfections within the material; it can only detect flaws that are close to the surface.
- Some forms of imperfections, such as fatigue cracks or microstructural defects, may be difficult to find with LPT.

## 6.8 Observations after Liquid Penetrate Testing

**Table 6.1 Observation after Liquid Penetrant Testing**

<b>Sr. No.</b>	<b>Test Specimen No.</b>	<b>Observation</b>
1	1	No Defects were Observed
2	2	No Defects were Observed
3	3	No Defects were Observed
4	4	No Defects were Observed
5	5	Defects were Observed at the edge of welding
6	6	No Defects were Observed
7	7	No Defects were Observed
8	8	No Defects were Observed
9	9	No Defects were Observed
10	10	No Defects were Observed
11	11	No Defects were Observed
12	12	No Defects were Observed
13	13	No Defects were Observed
14	14	No Defects were Observed
15	15	Defects were Observed at the edge of welding
16	16	No Defects were Observed
17	17	No Defects were Observed
18	18	No Defects were Observed
19	19	No Defects were Observed
20	20	No Defects were Observed



## 6.9 Hardnesstesting<sup>[5]</sup>:



**Fig 6.12 Hardness testing machine**



**Fig 6.13 Performing Hardness Test**

- Any material's hardness is determined by its resistance to friction, often known as abrasion. In order to determine whether a material is strong enough to withstand the force of an external load placed on a weld joint, hardness is primarily measured.
- According to ASTM standard E18 for the Rockwell hardness test, the test is conducted.
- The hardness testing machine used to assess the hardness of welded specimens is shown in the above-mentioned Fig. 6.11 and is located in the lab at our university.
- This Rockwell hardness tester uses an application load of 100KN for aluminum.
- On this machine, all hardness testing procedures are performed manually while being observed by a guide.
- The table contains a list of all specimens' hardness testing results.

## 6.10 Tensile testing

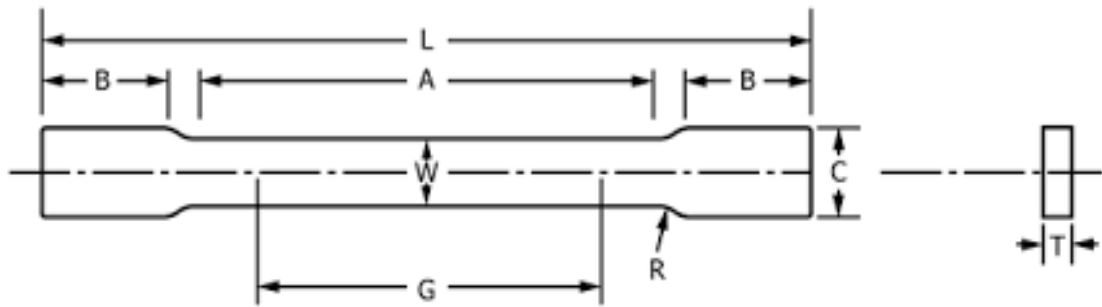


Fig 6.14 Tensile test specimen ASTM 370 standard<sup>[10]</sup>

- The civil engineering lab at our university provides tensile testing on welded specimens.
- The universal testing machine is utilized for tensile testing.
- Tensile tests are conducted as specified by ASTM standard A370.
- The tensile test specimen for this standard workpiece has been manufactured in accordance with the standard specimen indicated in Fig.6.13.



Fig 6.15 Preparing tensile test specimen using a Hacksaw cutting machine

- Fig.6.14 shows the preparing tensile specimen using a hacksaw cutting machine according to the ASTM standard A370 respectively.
- This machine has the ability to cutting tensile test specimens as per ASTM standard A370.
- A hacksaw cutting machine is a machine tool used for cutting materials such as metal, plastic, or wood. It uses a reciprocating saw blade that is powered by an electric motor to cut through the material.

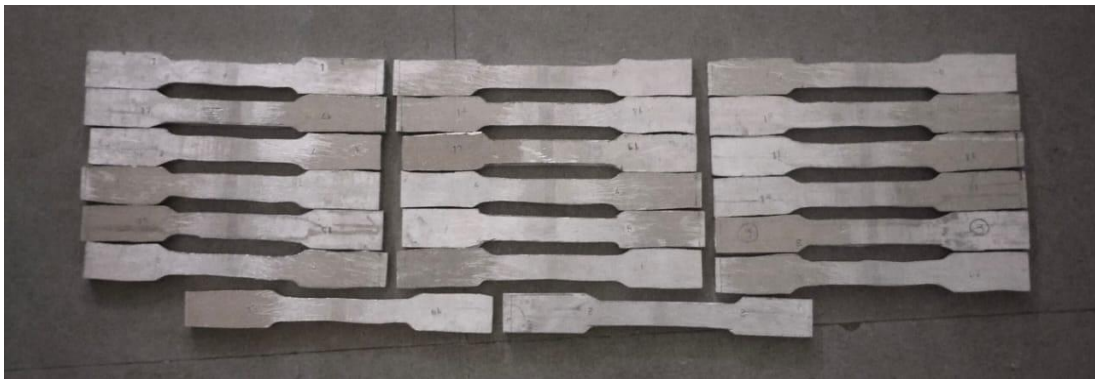


**Fig 6.16 Tensile test specimen**



**Fig 6.17 Tensile testing on UTM**

**Fig 6.18 Performing tensile testing**

- After performing the tensile testing on the Universal testing machine, the table contains a list of all specimens' tensile testing results.

**CHAPTER - 7**  
**RESULTS AND DISCUSSION**

**7.1 Actual experiment results:**

**7.1.1 Liquid penetrant test result**

**Table 7.1 Result of Liquid Penetrant Testing**

Sr. No.	Test Specimen No.	Observation
1	1	No Defects were Observed
2	2	No Defects were Observed
3	3	No Defects were Observed
4	4	No Defects were Observed
5	5	Defects were Observed at the edge of welding
6	6	No Defects were Observed
7	7	No Defects were Observed
8	8	No Defects were Observed
9	9	No Defects were Observed
10	10	No Defects were Observed
11	11	No Defects were Observed
12	12	No Defects were Observed
13	13	No Defects were Observed
14	14	No Defects were Observed
15	15	Defects were Observed at the edge of welding
16	16	No Defects were Observed
17	17	No Defects were Observed
18	18	No Defects were Observed
19	19	No Defects were Observed
20	20	No Defects were Observed

7.1.2 Hardness test result

Table 7.2hardness test result

Sr. No.	Parameters			Hardness (HRC)			
	Peak current (Ip)	Base current (Ib)	Pulse per second (Hz)	Weld zone (WZ)			
				Top	Center	Bottom	Average
1.	160	80	110	52	56	54	54
2.	160	80	150	56	55	57	56
3.	160	90	130	55	57	56	56
4.	160	100	110	59	58	57	56
5.	160	100	150	58	60	61	60
6.	180	80	130	60	61	63	62
7.	180	90	110	61	63	60	62
8.	180	90	130	60	64	63	63
9.	180	90	130	61	63	63	63
10.	180	90	130	62	64	65	64
11.	180	90	130	62	65	64	66
12.	180	90	130	65	69	68	68
13.	180	90	130	69	72	70	70
14.	180	90	150	72	73	71	72
15.	180	100	130	72	75	72	73
16.	200	80	110	78	76	77	77
17.	200	80	150	80	83	83	82
18.	200	90	130	85	87	86	85
19.	200	100	110	88	89	91	90
20.	200	100	150	90	96	95	94

7.1.2.1 3D Surface plot for hardness

Factor Coding: Actual


3D Surface

**hardness (HRC)**

Design Points:

● Above Surface

○ Below Surface

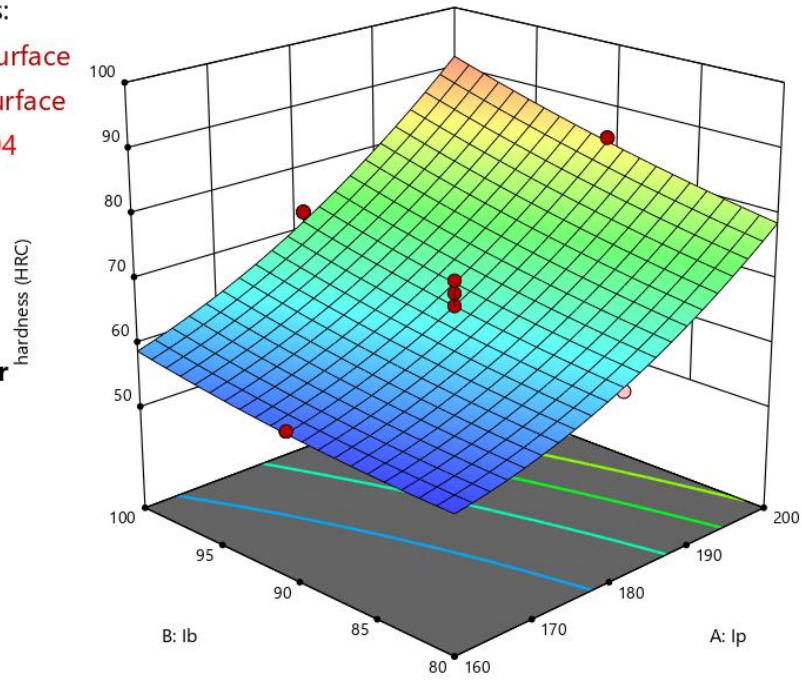
54  94

X1 = A

X2 = B

**Actual Factor**

C = 130



7.1.3 Tensile test result

Table 7.3 Tensile test result

Sr. No.	Peak current (Ip)	Base current (Ib)	Pulse per second (Hz)	Tensile load (KN)	Tensile strength (Mpa)
1.	160	80	110	14.99	133.84
2.	160	80	150	16.33	136.08
3.	160	90	130	15.73	140.45
4.	160	100	110	15.09	145.10
5.	160	100	150	16.41	157.79
6.	180	80	130	16.96	151.43
7.	180	90	110	17.66	157.68
8.	180	90	130	17.82	159.11
9.	180	90	130	17.77	148.08
10.	180	90	130	17.84	148.67
11.	180	90	130	17.79	158.84
12.	180	90	130	17.82	159.11
13.	180	90	130	17.78	158.75
14.	180	90	150	17.89	159.73
15.	180	100	130	18.01	173.17
16.	200	80	110	19.34	185.96
17.	200	80	150	18.96	169.29
18.	200	90	130	19.11	170.63
19.	200	100	110	21.03	202.21
20.	200	100	150	21.33	205.10



7.1.3.1 3d surface plot of peak current and base current for tensile

Factor Coding: Actual


3D Surface

**tensile (Mpa)**

Design Points:

● Above Surface

○ Below Surface

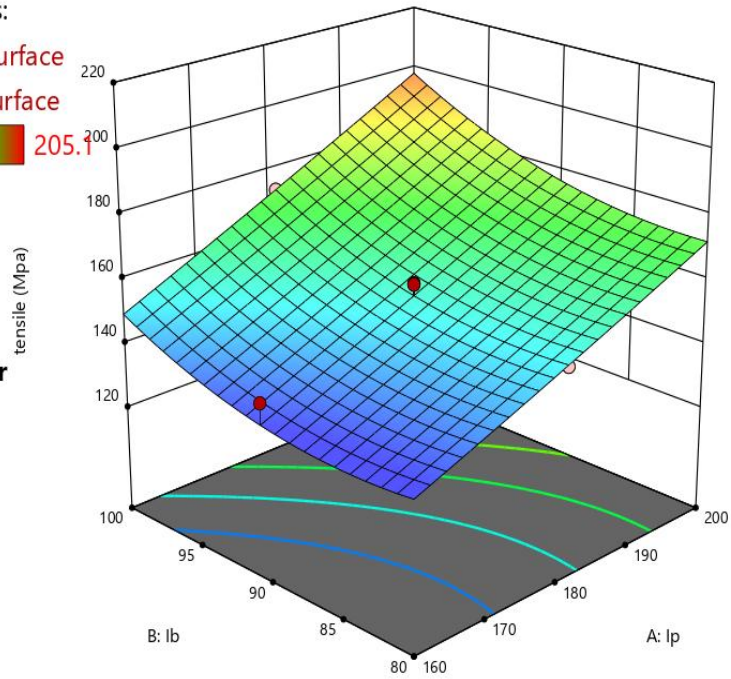
133.84  205.1

X1 = A

X2 = B

**Actual Factor**

C = 130





7.1.3.2 3d surface plot of peak current and pulse per second for tensile

Factor Coding: Actual

3D Surface

**tensile (Mpa)**

Design Points:

● Above Surface

○ Below Surface

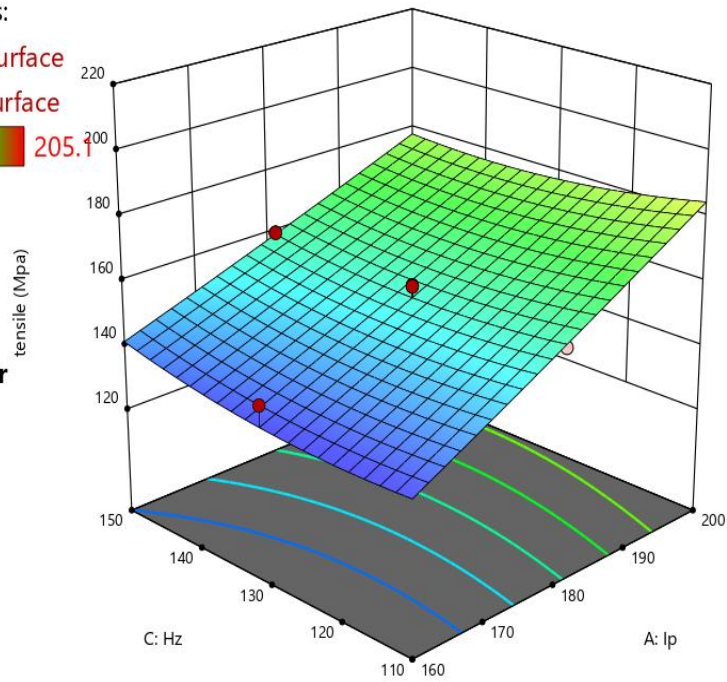
133.84  205.7

X1 = A

X2 = C

**Actual Factor**

B = 90



7.1.3.3 3d surface plot of base current and pulse per second for tensile

Factor Coding: Actual

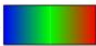
3D Surface

tensile (Mpa)

Design Points:

● Above Surface

○ Below Surface

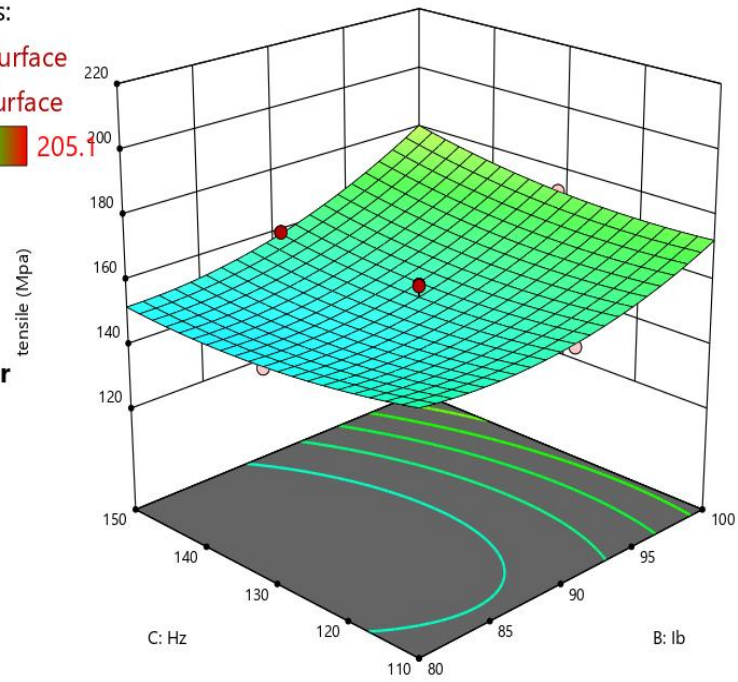
133.84  205.1

X1 = B

X2 = C

Actual Factor

A = 180



## CHAPTER - 8

# OPTIMIZATION AND VALIDATION

---

### 8.1 Optimization using response surface method

Response Surface Method (RSM) is a statistical method used for optimization when the response variable is influenced by several input variables. RSM involves constructing a mathematical model that relates the response variable to the input variables, and then optimizing the response variable using the model.

The basic steps involved in RSM optimization are:

**Experimental Design:** The first step in RSM is to design a set of experiments to obtain data on the response variable and the input variables. A common design used in RSM is the central composite design (CCD), which involves selecting a set of experimental points that are equidistant from a central point.

**Model Development:** The next step is to develop a mathematical model that relates the response variable to the input variables. The most common models used in RSM are polynomial models, which are based on second-order or higher-order equations.

**Model Fitting:** The model is fitted to the experimental data to estimate the model parameters.

**Model Validation:** The model is validated by comparing the predicted values with the actual experimental values.

**Optimization:** Once the model has been validated, it can be used to optimize the response variable. This involves finding the input variables that will maximize or minimize the response variable, subject to any constraints.

RSM has several advantages, including:

It can handle multiple input variables and complex interactions between them.

It can reduce the number of experiments required to obtain accurate results.

It provides a mathematical model that can be used to predict the response variable for new input values.

However, RSM also has some limitations, including:

It assumes that the response variable is a continuous function of the input variables.

It assumes that the input variables are independent and normally distributed.

It can be computationally intensive to fit and optimize the model.

Overall, RSM is a powerful tool for optimization when multiple input variables are involved. It can help reduce the number of experiments required and provide a mathematical model that can be used for prediction and optimization.

## **8.2 Experimental design**

Designing a number of experiments that collect information on the response variable and the input variables is the first step in RSM. The central composite design (CCD), which involves selecting a group of experimental points that have equal distances from a central point, is frequently used in RSM. The design of experiment using central composite design which is already mentioned in table

## **8.3 Model fitting**

Model fitting in regression analysis refers to the process of estimating the parameters of a regression model using available data. The goal is to find the best-fitting model that accurately captures the relationship between the dependent variable and the independent variables.

### **8.3.1 Regression analysis**

Regression analysis is a statistical method used to investigate the relationship between a dependent variable and one or more independent variables. It aims to understand how changes in the independent variables are associated with changes in the dependent variable. Regression analysis is commonly employed for predictive modeling, forecasting, and understanding the causal relationships between variables.

In regression analysis, the dependent variable is the outcome or response variable that we want to predict or explain. The independent variables, also known as predictor variables or regressors, are the variables used to predict or explain the variation in the dependent variable. The relationship between the dependent variable and the independent variables is typically represented by a mathematical equation called the regression model.

The regression model can take different forms depending on the nature of the data and the research question. The simplest form is the linear regression model, where the relationship between the variables is assumed to be linear. The linear regression model can be expressed as:

$$Y = \beta_0 + \beta_1 X_1 + \beta_2 X_2 + \dots + \beta_n X_n + \varepsilon$$

In this equation, Y represents the dependent variable, X<sub>1</sub>, X<sub>2</sub>, ..., X<sub>n</sub> represent the independent variables, β<sub>0</sub>, β<sub>1</sub>, β<sub>2</sub>, ..., β<sub>n</sub> are the regression coefficients that quantify the relationship between the variables, and ε represents the error term or residual, which captures the unexplained variation in the dependent variable.

The goal of regression analysis is to estimate the regression coefficients that best fit the data, meaning that they minimize the difference between the observed values of the dependent variable and the predicted values from the model. This estimation process is typically done using methods such as ordinary least squares (OLS), maximum likelihood estimation (MLE), or other specialized techniques depending on the specific requirements of the analysis.

Regression analysis provides various insights and outputs. The estimated coefficients can be interpreted to understand the magnitude and direction of the relationship between the variables. Statistical tests can be performed to assess the significance of the coefficients and determine if the independent variables have a significant impact on the dependent variable. Additionally, regression analysis can provide measures of goodness of fit, such as R-squared, adjusted R-squared, and standard error of the estimate, to evaluate the overall performance of the model.

Overall, regression analysis is a powerful tool for exploring and quantifying relationships between variables, making predictions, and understanding the factors that influence the outcome of interest. It finds applications in various fields such as economics, finance, social sciences, engineering, and healthcare, among others.

### 8.3.2 Regression Equation of Hardness

$$\text{Hardness} = 509.35 + -4.03938 * \text{Peak current} + -3.19125 * \text{Base current} + -0.435 * \text{Pulse per second} + 0.010625 * \text{Peak current} * \text{Base current} + 0.0015625 * \text{Peak current} * \text{Pulse per second} + -0.000625 * \text{Base current} * \text{Pulse per second} + 0.01 * \text{Peak current}^2 + 0.01 * \text{Base current}^2 + 0.00125 * \text{Pulse per second}^2$$

The equation in terms of actual factors can be used to make predictions about the response for given levels of each factor. Here, the levels should be specified in the original units for each factor. This equation should not be used to determine the relative impact of each factor because the coefficients are scaled to accommodate the units of each factor and the intercept is not at the center of the design space.

### 8.3.3 Regression Equation of Tensile

$$\text{Tensile} = 857.684 + 0.687772 * \text{Peak current} + -16.6951 * \text{Base current} + -2.47867 * \text{Pulse per second} + 0.0119313 * \text{Peak current} * \text{Base current} + -0.00897187 * \text{Peak current} * \text{Pulse per second} + 0.0187563 * \text{Base current} * \text{Pulse per second} + 0.00140114 * \text{Peak current}^2 + 0.0732045 * \text{Base current}^2 + 0.00931364 * \text{Pulse per second}^2$$

The equation in terms of actual factors can be used to make predictions about the response for given levels of each factor. Here, the levels should be specified in the original units for each factor. This equation should not be used to determine the relative impact of each factor because the coefficients are scaled to accommodate the units of each factor and the intercept is not at the center of the design space.

## 8.4 Model analysis

Model analysis in response surface methodology (RSM) refers to the process of evaluating the fitted model to determine its accuracy and effectiveness in predicting the response variable. The main objective of model analysis is to assess the quality of the fitted model and identify any significant factors or interactions that affect the response variable.

### 8.4.1 ANOVA for hardness (WZ)

**Table 8.2 ANOVA for hardness (WZ)**

Source	Sum of Squares	df	Mean Square	F-value	p-value
<b>Model</b>	2484.72	9	276.08	42.46	< 0.0001
A-1p	2073.60	1	2073.60	318.89	< 0.0001
B-1b	193.60	1	193.60	29.77	0.0003
C-Hz	52.90	1	52.90	8.14	0.0172
AB	36.12	1	36.12	5.56	0.0402
AC	3.12	1	3.12	0.4806	0.5039
BC	0.1250	1	0.1250	0.0192	0.8925
A <sup>2</sup>	44.00	1	44.00	6.77	0.0264
B <sup>2</sup>	2.75	1	2.75	0.4229	0.5301
C <sup>2</sup>	0.6875	1	0.6875	0.1057	0.7518
<b>Residual</b>	65.02	10	6.50		
Lack of Fit	23.69	5	4.74	0.5732	0.7219
Pure Error	41.33	5	8.27		
<b>Cor Total</b>	2549.75	19			
<b>Fit summary</b>					
Model degree	Quadratic – significant				
R <sup>2</sup>	0.9745				
Adjusted R <sup>2</sup>	0.9515				
Predicted R <sup>2</sup>	0.9095				

The Model F-value of 42.46 implies the model is significant. There is only a 0.01% chance that an F-value this large could occur due to noise.

P-values less than 0.0500 indicate model terms are significant. In this case A, B, C, AB, A<sup>2</sup> are significant model terms. Values greater than 0.1000 indicate the model terms are not significant. If there are many insignificant model terms (not counting those required to support hierarchy), model reduction may improve your model.

The Lack of Fit F-value of 0.57 implies the Lack of Fit is not significant relative to the pure error. There is a 72.19% chance that a Lack of Fit F-value this large could occur due to noise. Non-significant lack of fit is good -- we want the model to fit.

### 8.4.2 ANOVA for tensile strength

**Table 8.3 ANOVA for tensile strength**

Source	Sum of Squares	df	Mean Square	F-value	p-value
<b>Model</b>	6778.78	9	753.20	26.81	< 0.0001
A- <i>I</i> <sub>p</sub>	4836.92	1	4836.92	172.16	< 0.0001
B- <i>I</i> <sub>b</sub>	1139.98	1	1139.98	40.58	< 0.0001
C- <i>H</i> <sub>z</sub>	1.02	1	1.02	0.0364	0.8524
AB	45.55	1	45.55	1.62	0.2317
AC	103.03	1	103.03	3.67	0.0845
BC	112.58	1	112.58	4.01	0.0732
A <sup>2</sup>	0.8638	1	0.8638	0.0307	0.8643
B <sup>2</sup>	147.37	1	147.37	5.25	0.0450
C <sup>2</sup>	38.17	1	38.17	1.36	0.2708
<b>Residual</b>	280.95	10	28.10		
Lack of Fit	131.50	5	26.30	0.8798	0.5541
Pure Error	149.46	5	29.89		
<b>Cor Total</b>	7059.73	19			
<b>Fit summary</b>					
Model degree	Quadratic – significant				
R <sup>2</sup>	0.9602				
Adjusted R <sup>2</sup>	0.9244				
Predicted R <sup>2</sup>	0.8056				

The Model F-value of 26.81 implies the model is significant. There is only a 0.01% chance that an F-value this large could occur due to noise.

P-values less than 0.0500 indicate model terms are significant. In this case A, B, B<sup>2</sup> are significant model terms. Values greater than 0.1000 indicate the model terms are not significant. If there are many insignificant model terms (not counting those required to support hierarchy), model reduction may improve your model.

The Lack of Fit F-value of 0.88 implies the Lack of Fit is not significant relative to the pure error. There is a 55.41% chance that a Lack of Fit F-value this large could occur due to noise. Non-significant lack of fit is good -- we want the model to fit.



### 8.5 Model optimization

Response Surface Methodology (RSM) is a statistical technique used to optimize a process with multiple variables by constructing a mathematical model that describes the relationship between the process variables and the response of interest. The optimization process involves finding the optimal combination of input variables that maximize or minimize the response.

**Table 8.4** Constraints in Optimization

Name	Goal	Lower Limit	Upper Limit
<b>Input parameters</b>			
A: Peak current (Ip)	is in range	160	200
B: Base current (Ib)	is in range	80	100
C: Pulse per second (Hz)	is in range	110	150
<b>Output parameters (Responses)</b>			
Tensile (N/mm <sup>2</sup> )	Maximize	133.84	205.1
Hardness (HRC)	Maximize	54	94

**Table 8.5** Suggested optimized solution

Input variables	Suggested results at optimum condition	Output variables	Suggested results at optimum condition
<b>Peak current (Amp)</b>	200	<b>Tensile strength (Mpa)</b>	202.393
<b>Base current (Amp)</b>	100	<b>Hardness (HRC)</b>	95.252
<b>Pulse per second (Hz)</b>	150		
<b>Desirability: 0.981</b>			

### 8.6 Validation of results

Validation of the results obtained from Response Surface Methodology (RSM) is a critical step to ensure the accuracy and reliability of the optimization process. The validation process involves evaluating the quality of the model and assessing its ability to predict the response under different scenarios.

**Table 8.6**Confirmation test results

<b>Input process parameter at optimum condition</b>							
<b>Peak current: 200Amp</b>		<b>Base current: 100 Amp</b>			<b>Pulse per second: 150 Hz</b>		
<b>Experimental results – output parameters</b>							
<b>Tensile Strength</b>	<b>Width (mm)</b>	<b>Thickness (mm)</b>	<b>Area (mm<sup>2</sup>)</b>	<b>Load (N)</b>	<b>Tensile strength (N/mm<sup>2</sup>)</b>	<b>Avg. tensile strength (Mpa)</b>	<b>Remarks</b>
		12.83	8	103.12	21030	203.94	203.94
<b>Hardness</b>	<b>Hardness at weld zone (WZ)</b>						<b>Avg. hardness (WZ)</b>
	<b>Top</b>		<b>Center</b>	<b>Bottom</b>			
	94	95	96	94	95	94.800	

**Table 8.7**Comparison of predicted result with experimental results

<b>Parameters</b>		<b>Predicted results at optimum condition</b>	<b>Experimental results</b>	<b>% of Deviation</b>
<b>Input</b>	<b>Peak current (Amp)</b>	200	200	
	<b>Base current (Amp)</b>	100	100	
	<b>Pulse per second (Hz)</b>	150	150	
<b>Output</b>	<b>Tensile strength (Mpa)</b>	202.393	203.940	0.46
	<b>WZ Hardness (HRC)</b>	95.252	94.800	0.21

## CHAPTER - 9

### CONCLUSIONS AND FUTURE SCOPE

#### 9.1 Conclusion

The following conclusion can be made listed below-

1. Peak current (A), Base current (A), and pulse per second (%) are the three parameters that have the greatest influence on the quality of welding, respectively.
2. With the optimization of input parameters the value achieved that are:  
 Peak current-200 A,  
 Base current - 100 A, and  
 Pulse Per Second- 150 Hz  
 gives the output parameters as  
 Tensile Strength- 205.10 MPa and  
 Hardness achieved for WZ- 94 (HRC).
3. It is observed that as the peak current increases tensile strength and hardness slightly increases.
4. It is clearly seen that when pulse on time increases hardness is slightly decreases but tensile strength slightly increases.
5. The optimum results obtained from experimentations are as follows

Peak Current = 200 A

Base Current = 100 A

Pulse Per Second = 150 Hz

Tensile strength = 202.393 MPa

Hardness (WZ) = 95.252 (HRC)

6. Experimental values after doing experiments on the basis of optimized value are as follows

Tensile strength= 203.940Mpa

Hardness (WZ)= 94.800

7. After comparing both the results the error found out to be

Tensile strength= 0.46%

Hardness (WZ)= 0.21%

## 9.2 Future scope

Based on the results of the present investigation, the following recommendations are given to investigate this area of PC TIG welding of aluminium alloys further.

1. For the research, a number of parameters such as welding speed, gas flow rate, frequency, etc., have an impact on the mechanical properties of the weld joint.
2. Different optimization software can be taken into consideration using optimised parameters.
3. Choose the other grades of aluminium alloys for PC TIG welding for additional investigation.

## REFERENCES

1. G. Mathers, The welding of aluminium and its alloys. New York: Woodhead Publishing Limited, 2002.
2. Davis, J. R. (1993). Aluminum and aluminum alloys. ASM international.
3. A.S.M.E. Section II A: Boiler, A. S. M. E., & Code, P. V. (2019). Section II Materials.Part A–Properties.
4. American Welding Society. (1950). Welding handbook (Vol. 1). American Welding Society.
5. American Society for Testing and Materials. Committee E-28 on Mechanical Testing. (2019). Standard test methods for rockwell hardness of metallic materials. ASTM International.
6. Sec II, A. S. M. E. (2004). Specification for Welding Rods, Electrodes and Filler Metals, Part C. American Society of Mechanical Engineers.
7. Wahid, M. A., Siddiquee, A. N., & Khan, Z. A. (2020). Aluminum alloys in marine construction: characteristics, application, and problems from a fabrication viewpoint. *Marine Systems & Ocean Technology*, 15(1), 70-80.
8. Montgomery, D. C. (2017). Design and analysis of experiments. John wiley & sons.
9. A.S.M.E. section V: Boiler, A.S.M.E., & Code, P.V.(2017). Section V Non- destructive examination.
10. ASTM, I. (2012). Standard test methods and definitions for mechanical testing of steel products. ASTM A370.
11. Yelamasetti, B., & Vardhan, V. (2021). Optimization of GTAW parameters for the development of dissimilar AA5052 and AA6061 joints. *Materials Today: Proceedings*, 47, 4350-4356.
12. Verma, S., Arya, H. K., & Kumar, P. Effect of Post Weld Heat Treatment on Properties of ACTIGWeldedAa6063 AluminiumAlloy Joint.
13. Arunkumar, K., & Dhayanithi, G. Analysis of Welding Characteristics in Aa 5052 Using GasTungstenArcWelding.
14. Parthasarathy, M.C., & Sathyaseelan,M.D. (2015). An Investigation on EffectofProcessParameterof Pulsed Tig WeldedAluminumAlloy onMechanicaland CorrosionProperties

15. Hong, S. M., Tashiro, S., Bang, H. S., & Tanaka, M. (2021). A Study on the Effect of Current Waveform on Intermetallics Formation and the Weldability of Dissimilar Materials Welded Joints (AA5052 Alloy—GI Steel) in AC Pulse GMAW. *Metals*, 11(4), 561.
16. Sanjeevi, C., & Muthukumar, k. (2020). improving welding joint strength with aluminium alloy 5052 using gas metal arc welding.
17. Hasanniah, A., & Movahedi, M. (2018). Welding of Al-Mg aluminium alloy to aluminium clad steel sheet using pulsed gas tungsten arc process. *Journal of Manufacturing Processes*, 31, 494-501.
18. Eazhil, K. M., Mahendran, S., & Kumar, S. G. (2014). Optimization of tungsten inert gas welding on 6063 aluminium alloy using Taguchi method. *Int J of Research and Scientific Innovations*, 1(3).
19. Yelamasetti, B., & Vardhan, V. (2021). Weldability and mechanical properties of AA5052 and AA7075 dissimilar joints developed by GTAW process. *Materials Today: Proceedings*, 47, 4162-4166.
20. Ramji, B. R., Bharathi, V., & Swamy, N. P. (2021). Characterization of TIG and MIG welded Aluminium 6063 alloys. *Materials Today: Proceedings*, 46, 8895-8899.
21. Yelamasetti, B., Kumar, D., & Saxena, K.K. (2021). Experimental investigation on temperature profiles and residual stresses in GTAW dissimilar weldments of AA5052 and AA7075. *Advances in Materials and Processing Technologies*, 1-1
22. Yelamasetti, B., Ramana G, V., Manikyam, S., & Vardhan T, V. (2021). Thermal field and residual stress analyses of similar and dissimilar weldments joined by constant and pulsed current TIG welding techniques. *Advances in Materials and Processing Technologies*, 1-16.
23. sandhya, v., sadaf, a., reddy, b. p., & priyanka, k. experimental investigations on effect of weld parameters in tig welding of aluminium.
24. Yan, Z., Yuan, T., & Chen, S. (2019). Microstructural refinement of 6061 and 5052 aluminium alloys by arc oscillation. *Materials Science and Technology*, 35(13), 1651-1655.
25. Kato, S., & Tanabe, S. (1988). High speed welding of 0.5 mm thickness alloy sheets using pulsed TIG welding. *welding International*, 2(7), 602-608.
26. Miniappan, P.K., Shankar, V.A., & Ibrahim, A.S. (2020). Anevaluation of microstructural effect on welding interface of welded samples. *Journal of Critical Reviews*, 7(9).
27. Chen, W.B. (2016). Microstructure and mechanical properties of tungsten inert gas welded-brazed Al/Ti joints. *Science and Technology of Welding and Joining*, 21(7), 547-554.

28. Raveendra, A., & Kumar, B. R. Effect of Pulsed Current on Welding Characteristics of Aluminium Alloy (5052) using Gas Tungsten Arc Welding.
29. Abioye, T. E., Zuhailawati, H., Aizad, S., & Anasyida, A. S. (2019). Geometrical, microstructural and mechanical characterization of pulse laser welded thin sheet 5052-H32 aluminium alloy for aerospace applications. *Transactions of Nonferrous Metals Society of China*, 29(4), 667-679.
30. Shrivastava, S. P., Vaidya, S. K., Khandelwal, A. K., & Vishvakarma, K. (2020). Investigation of TIG welding parameters to improve strength. *Materials Today: Proceedings*, 26, 1897-1902.
31. Ye, Z., Huang, J., Gao, W., Zhang, Y., Cheng, Z., Chen, S., & Yang, J. (2017). Microstructure and mechanical properties of 5052 aluminum alloy/mild steel butt joint achieved by MIG-TIG double-sided arc welding-brazing. *Materials & Design*, 123, 69-79.
32. Song, C. Y., Park, Y. W., Kim, H. R., Lee, K. Y., & Lee, J. (2008). The use of Taguchi and approximation methods to optimize the laser hybrid welding of a 5052-H32 aluminium alloy plate. *Proceedings of the Institution of Mechanical Engineers, Part B: Journal of Engineering Manufacture*, 222(4), 507-518.
33. Yelamasetti, B., & Vardhan, V. (2021). Weldability and mechanical properties of AA5052 and AA7075 dissimilar joints developed by GTAW process. *Materials Today: Proceedings*, 47, 4162-4166.
34. Shanavas, S., & Dhas, J. E. R. (2017, October). Weldability of AA 5052 H32 aluminium alloy by TIG welding and FSW process—a comparative study. In *IOP Conference Series: Materials Science and Engineering* (Vol. 247, No. 1, p. 012016). IOP Publishing.
35. Shunmugasundaram, M., Kumar, A. P., Sankar, L. P., & Sivasankar, S. (2020). Optimization of process parameters of friction stir welded dissimilar AA6063 and AA5052 aluminum alloys by Taguchi technique. *Materials Today: Proceedings*, 27, 871-876.
36. Baskoro, A. S., Amat, M. A., Pratama, I., Kiswanto, G., & Winarto, W. (2019). Effects of tungsten inert gas (TIG) welding parameters on macrostructure, microstructure, and mechanical properties of AA6063-T5 using the controlled intermittent wire feeding method. *The International Journal of Advanced Manufacturing Technology*, 105(5), 2237-2251.
37. Hadadzadeh, A., Ghaznavi, M. M., & Kokabi, A. H. (2014). The effect of gas tungsten arc welding and pulsed-gas tungsten arc welding processes' parameters on the heat affected zone-



- softening behavior of strain-hardened Al–6.7Mg alloy. *Materials & Design*, 55,335-342.
38. Reddy, G. M., Gokhale, A. A., & Rao, K. P. (1998). Optimisation of pulse frequency in pulsed current gas tungsten arc welding of aluminium– lithium alloy sheets. *Materials Science and Technology*, 14(1), 61-66.
  39. Verma, R. P., Pandey, K. N., & Sharma, Y. (2015). Effect of ER4043 and ER5356 filler wire on mechanical properties and microstructure of dissimilar aluminium alloys, 5083-O and 6061-T6 joint, welded by the metal inert gas welding. *Proceedings of the Institution of Mechanical Engineers, Part B: Journal of Engineering Manufacture*, 229(6), 1021-1028.
  40. Praveen, P., & Yarlagadda, P. K. D. V. (2005). Meeting challenges in welding of aluminum alloy through pulse gas metal arc welding. *Journal of Material*.
  41. Ravendra, A. (2014). Effect of welding parameters on weld characteristics of 5052 Aluminium Alloy sheet using TIG Welding. *International Journal of Innovative Research in Science, Engineering and Technology*, 3(3), 10302-10309.
  42. Feng, Z. (1994). A computational analysis of thermal and mechanical conditions for weld metal solidification cracking. *WELDING IN THE WORLD-LONDON-*, 33, 340-340.
  43. Chand, A.G., & Yadav, S.K. (2018). EXPERIMENTAL INVESTIGATION OF WELD JOINT OF TUNGSTEN INERT GAS WELDING (TIG) ON ALUMINIUM ALLOY. *Journal of emerging technologies and innovative research*.
  44. Raveendra, A., Kumar, D. B. R., Sivakumar, A., & Reddy, V. P. (2014). Influence of Welding Parameters on Weld Characteristics of 5052 Aluminium Alloy sheet Using TIG Welding. *International Journal of Application or Innovation in Engineering & Management (IJAIEM)*, 3(3).
  45. Raveendra, A., & Tjprc (2018). Micro-Hardness and Mechanical Properties of 5052 Aluminium Alloy Weldments Using Pulsed and Non-Pulsed Current Gas Tungsten ARC Welding.
  46. Kumar, A., & Sundarajan, S. (2009). Optimization of pulsed TIG welding process parameters on mechanical properties of AA 5456 Aluminum alloy weldments. *Materials & Design*, 30(4), 1288-1297.
  47. Bajpei, T., Chelladurai, H., & Ansari, M. Z. (2016). Numerical investigation of transient temperature and residual stresses in thin dissimilar aluminium alloy plates. *Procedia Manufacturing*, 5, 558-567.
  48. Sharma, A. D., & Sharma, R. K. Aluminum Alloys Welding: A Review.

49. Okubo, M., & Takenaka, K. (1997). Dissimilar joints between Al-Mg A5052 wrought alloy and AC7A castings made by electron beam and gas tungsten arc welding. *Welding international*, 11(5), 346-352.

50.